DIRECT SYNTHESIS OF 2-METHYL-1-PROPANOL/METHANOL FUELS AND FEEDSTOCKS

Technical Progress Report for the Period

March - May 1985

DOE/PC/70021--2

DE89 008258

Kamil Klier
Richard G. Herman
Gary W. Simmons

with: Paul B. Himelfarb
John Nunan
Victor Kuzmicz

Center for Surface and Coatings Research
and
Department of Chemistry
LEHIGH UNIVERSITY
Bethlehem, PA 18015

June 1985

PREPARED FOR THE UNITED STATES
DEPARTMENT OF ENERGY

Under Contract No. **DE-AC22-84PC70021**

DIRECT SYNTHESIS OF 2-METHYL-1-PROPANOL/METHANOL FUELS AND FEEDSTOCKS

DIRECT SYNTHESIS OF 2-METHYL-1-PROPANOL/METHANOL FUELS AND FEEDSTOCKS

OBJECTIVES AND SCOPE OF WORK

The objective of this research project is to provide a technological and scientific foundation for the synthesis of 2-methyl-1-propanol/methanol fuels and basic chemicals from synthesis gas. These mixtures are excellent high octane fuels, can be blended with hydrocarbon gasoline, have high energy densities in the 2-methyl-1-propanol portion, and have synthesis stoichiometries that can be adjusted to the various H_2/CO ratios produced by different gasifiers and feedstocks.

The two principal tasks involve the following lines of research:

(i) the development and optimization of Cs/Cu/ZnO support catalysts wherein the cesium component provides a very effective basic function that steers the synthesis toward 2-methyl-1-propanol, and

(ii) the development of a kinetic reaction network that will be usable for reactor design, as well as for predictions of reaction conditions that give rise to the required 2-methyl-1-propanol/methanol composition in the reactor exit stream.

Auxiliary tasks of this research project that will utilize and build upon the data and principles derived from the two primary tasks deal with

(iii) providing mechanistic input into the kinetic modelling scheme based on experimental research using chemical trapping of surface intermediates, isotopic studies, and insitu infrared spectroscopy,

(iv) exploratory research into novel basic components, consisting of aluminosilicates and amines, that promote branching during carbon-carbon bond formation, and

(v) concurrent characterization of the catalysts by gaseous chemisorption techniques and by utilizing the modern techniques of HR-TEM, STEM, electron and X-ray diffraction, X-ray photoelectron spectroscopy, and vibrational spectroscopies such as laser Raman microprobe spectroscopy.

SUMMARY OF PROGRESS

The purpose of the work described in this report was to characterize in detail the promotional effect of Cs doping of the binary 30/70 Cu/ZnO catalyst for the synthesis of methanol and higher alcohols. This was done with the aim of laying a firm foundation for further studying the effect of the addition of a fourth component, aluminum, to the catalyst composition with the expressed aim of further increasing the catalyst stability under higher alcohol synthesis conditions.

To accomplish the above task, the following parameters were studied in detail:

(i) establish at what stage in catalyst preparation does Cs doping best promote methanol/higher alcohol synthesis, i.e. after calcination of the precursor aurichalcite to CuO/ZnO or after reduction of CuO/ZnO to Cu/ZnO.

(ii) at what doping level is maximum catalytic activity observed and is a shart maximum or a plateau observed in activity vs Cs doping level. This latter point is important since it will demonstrate whether or not the catalyst can be over-doped with Cs without the detrimental effect of loss of activity.

(iii) examine the long term stability of the Cs/Cu/ZnO catalyst under higher alcohol synthesis conditions.

(iv) to characterize in detail the catalyst morphology including catalyst surface area, crystallite sizes and the state of Cs (location and the degree of dispersion) before and after catalyst testing. This was done in an attempt to predict the enhanced catalytic activity based on the location and state of Cs on the catalyst surface.

In the present study the promotional effect of Cs was studied under reaction conditions where mass and heat transfer within the catalyst bed were not greatly affecting the overall reaction rate, thus allowing the true measure of Cs promotion to be determined. The products observed included methanol, methyl-formate, ethanol, and traces of carbon dioxide, water, and methane. Although higher molecular weight alcohols are the more desired products, analysis of the C_1-C_2 products formed does give a measure of the promotional effect for methanol formation and also for C-O (methyl-formate) and C-C (ethanol) bond formation.

It was observed that methanol, ethanol, and methyl-formate synthesis rates were dramatically increased by surface doping of both reduced Cu/ZnO and calcined CuO/ZnO catalysts with CsOOCH. The promotion effect of Cs on the synthesis rates of the individual products followed the order ethanol>methyl-formate>methanol. Quantitative surface analysis showed that the Cs was atomically dispersed, primarily over the ZnO phase. The activity and selectivity of the catalyst was shown to be a function of Cs coverage. The maximum promotion effect occurred at different Cs coverages (Θ_{Cs}) for the different products, i.e. maximum methanol yield at Θ_{Cs} = 0.12, maximum methyl-formate formation at Θ_{Cs} = 0.19, and maximum ethanol production at Θ_{Cs} = 0.31.

Part B of this report details progress in developing a simplified high resolution analytical procedure for quantiatively determining the alcohols, esters, and ketones formed during the synthesis of higher molecular weight alcohols from synthesis gas. A method has been developed for these analyses using a wide bore bonded methyl silicone capillary column.

TECHNICAL PROGRESS

A. Characterization of Cs/Cu/ZnO Catalysts

EXPERIMENTAL

Catalyst Preparation. Catalysts having a composition of Cu/ZnO equal to 30/70 mol% were prepared according to the procedures given previously (1) The preparation included coprecipitation from nitrate solution, stepwise calcination of the precipitate to 350°C, pellitization of the CuO/ZnO, and reduction of the catalyst in 2% H_2/N_2 at 250°C.

The catalysts were doped after calcination or reduction with CsOOCH (Alfa Products) contained in an aqueous solution. The "reduced-doped" catalysts were prepared by removing the reduced catalyst (Cu/ZnO) from the reactor under N_2 and adding 2.5 g to 25 ml of N_2 purged CsOOCH solution at 50°C. The solution was then evaporated to dryness under flowing N_2, and the resulting doped catalyst was transported under N_2 into the reactor for activity testing. In this manner, reduced-doped catalysts were prepared having a Cs concentration of 0.10 to 0.80 mol%.

"Calcined-doped" catalysts were prepared by doping after calcination using the same procedure as described above. After doping, the catalysts were transported in air into the reactor for reduction followed by activity testing. Calcined-doped catalysts were prepared with 0.15 to 2.00 mol% Cs. The stock CsOOCH solution was analyzed by Galbraith Laboratories, Inc. for elemental concentration, and 86% of the expected Cs concentration was found. The uncertainty in the Cs concentration in the doped catalysts was $\pm$ 0.05 mol%, as determined by comparisons between the expected Cs/Cu/Zn concentrations and those obtained by Galbraith Laboratories.

Synthesis Activities. The catalysts were tested in a fixed bed flow reactor, which has been described in detail earlier (1). The synthesis products were analyzed by an on-line Hewlett-Packard 5730A gas chromatograph. Catalyst activities were determined at 250°C and 75 atm with a H_2/CO = 70/30 vol% synthesis gas with GHSV = 5000 hr^{-1} (15 l/hr with 3.0 ml portions of catalysts). Additionally, the product dependence on flow rate was determined using reactant gas flow rates from 2-40 l/hr at a temperature of 210°C, conditions which produced carbon conversion to methanol from 2.5 to 37.5 mol%.

After activity testing, the used catalysts were taken out of the reactor under N_2 and immediately stored under vacuum without exposure to air. The samples remained under vacuum until characterization studies commenced.

Catalyst Characterization. Powder X-ray diffraction patterns were obtained with a Philips XRG 3100 X-ray generator coupled with an APO 3600 control unit, using Cu K_α radiation. Scans were conducted with a step size of 0.01^o in 2θ and a counting time of 1.0 sec. The air sensitive samples were loaded into an air-tight sample holder under N_2, equipped with a beryllium window. Particle dimensions were approximated using the Sherrer equation (2) in the form of $d = 0.89\lambda/\cos(w_x^2 - w_o^2)$, where θ is the Bragg angle, w_x the measured half-width, w_o the instrumental half-width, and λ the X-ray wavelength, 0.15416 nm. For ZnO, the average particle dimension from the {100}, {002}, and {101} reflections is reported and for Cu the {111} reflection is given.

Surface areas were determined by the BET method using argon gas. Air sensitive samples were loaded under N_2 into the testing apparatus, evacuated overnight, and heated under vacuum for one hr at 110°C prior to surface area measurement. The experimental uncertainty in the surface area measurement was $\mp$ 3%.

Surface analyses were performed in a Physical Electronics 548 X-ray photoelectron spectrometer, having a Mg X-ray source. A 50 eV pass energy and scan rate of 0.2 eV/sec was used in the required 20 eV range for recording intensities of the $Zn2p_{3/2}$, $Cu2p_{3/2}$, and $Cs3d_{5/2}$ photoelectron lines. Signal averaging techniques were employed with the use of a Nicolet computer, Model 1072, multichannel analyzer. Integrated intensities were obtained with a Zeiss MOP-3 automatic integrator, and the background intensity correction was determined experimentally from an undoped sample. Quantitative surface analysis was accomplished using the method described in the Appendix.

RESULTS

Catalyst Activities. Rates of methanol formation over calcined- and reduced Cs-doped Cu/ZnO are shown in Figure 1. The different preparations produced identically active catalysts. An enhancement of over twofold in methanol yield was observed with a Cs concentration of 0.40 mol%. Increasing the Cs up to 1.0 mol% had little effect, but at higher concentrations, 2.0 mol%, the activity decreased to 85% the maximum value. The synthesis rates of ethanol and methyl-formate as a function of Cs concentration are presented in Figure 2. A dramatic enhancement was observed for both products.

Figure 1.

Yield of methanol as a function of Cs loading over the calcined-doped and reduced-doped catalysts. T = 250°C; H_2/CO = 2.333; P = 75 atmospheres; Feed of CO + H_2 = 15 ℓ/hr.

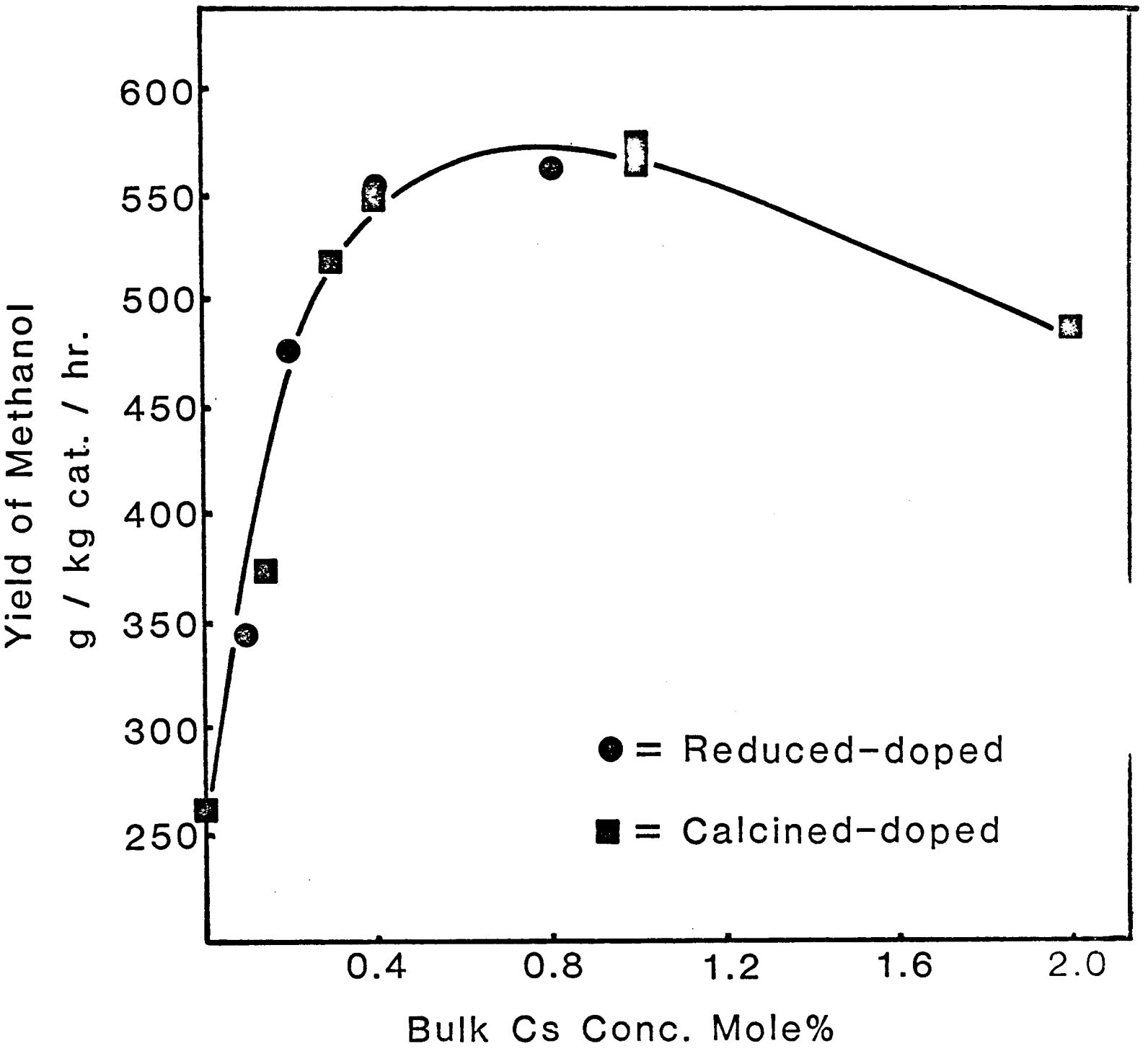

Figure 2.

Yields of methyl formate and ethanol as a function of Cs loading of the calcined-doped catalysts. T = 250°C; H_2/CO = 2.333; P = 75 atmospheres; Feed of CO + H_2 = 15 ℓ/hr.

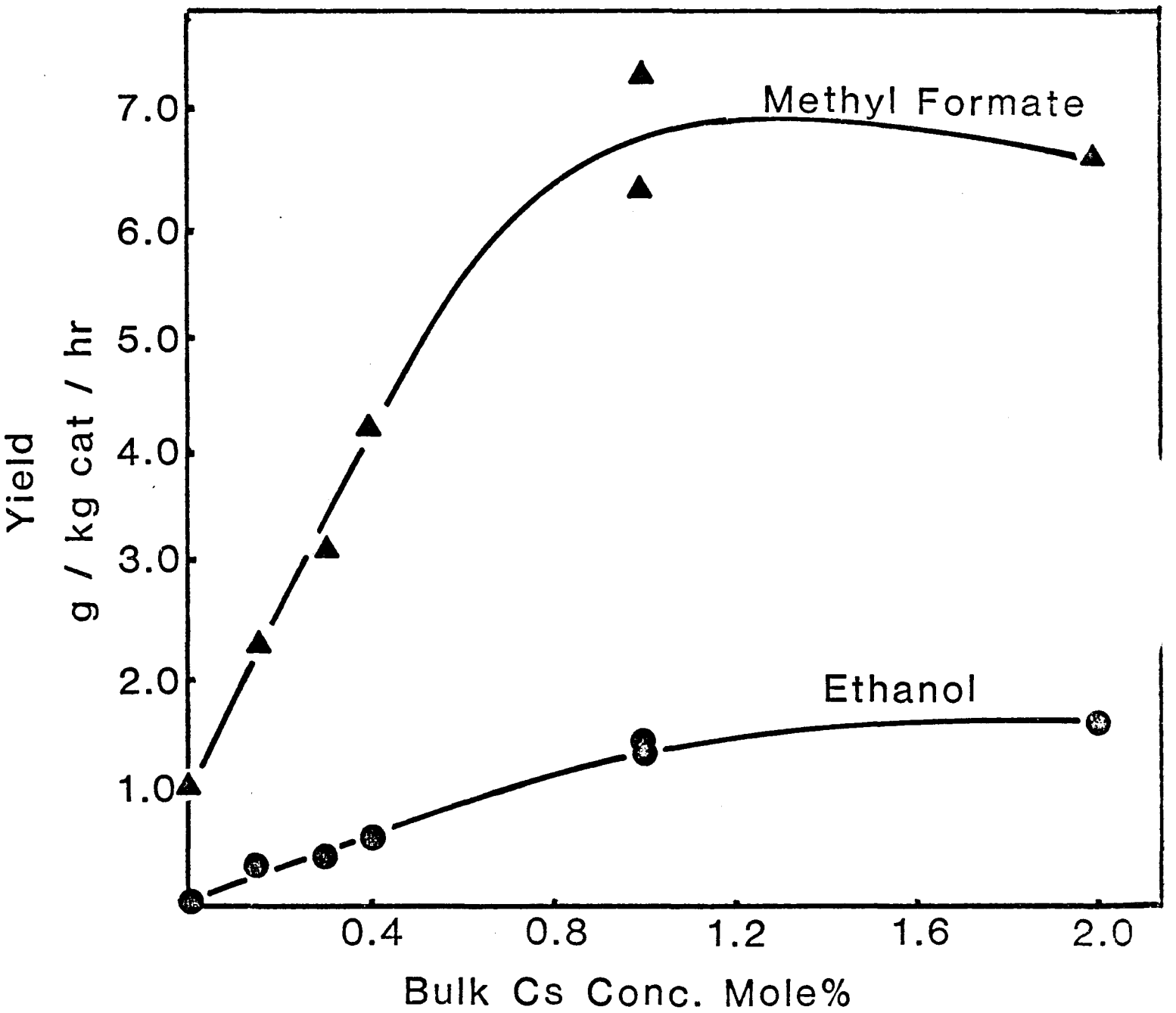

For methyl-formate, a plateau occurred in the synthesis rate with approximately 1.0 mol% Cs, and for ethanol the yield continually increased up to 2.0 mol% Cs.

The degree of methanol conversion as a function of reciprocal space velocity (proportional to contact time) is shown in Figure 3. The linear relationship over the carbon monoxide-to-methanol conversion range of 2-37.5 mol%, indicates that the reactor was operating under differential conditions in this range and that external mass transfer within the bed was not greatly affecting the rate. Thus, under these conditions the observed degree of conversion gives a direct measure of the reaction rate and the promotion effect of Cs.

Catalyst Characterization. ZnO and Cu particle dimensions determined by X-ray diffraction line broadening, and BET surface areas for the calcined-doped catalysts are given in Table 1. A linear relationship between the surface areas of the tested and untested catalysts was observed, and is shown graphically in Figure 4. The surface area changes in the doped tested catalysts were small, ranging from 37.8 m^2/g for the undoped catalyst to 32.4 m^2/g for the 1.0 mol% Cs sample.

The tested and untested samples were analyzed for surface elemental distribution using X-ray photoelectron spectroscopy (XPS), by the method described in the Appendix. A representative spectrum of a tested calcined-doped (0.4 mol% Cs) sample is given in Figure 5. The $Cs3d_{5/2}$, $Zn2p_{3/2}$, and $Cu2p_{3/2}$ photoelectron lines used in the analyses are identified.

In the analysis of the tested catalysts, elemental quantification of surface Cs was accomplished by using the Zn atom intensity as an internal reference. The Cu signal was not used because its degree of

Figure 3.

Effect of reciprocal space velocity on the activity for methanol formation over a 0.4 mol% Cs, calcined-doped catalyst.
T = 210°C; catalyst weight = 2.45 g; P = 75 atmospheres; H_2/CO = 2.333.

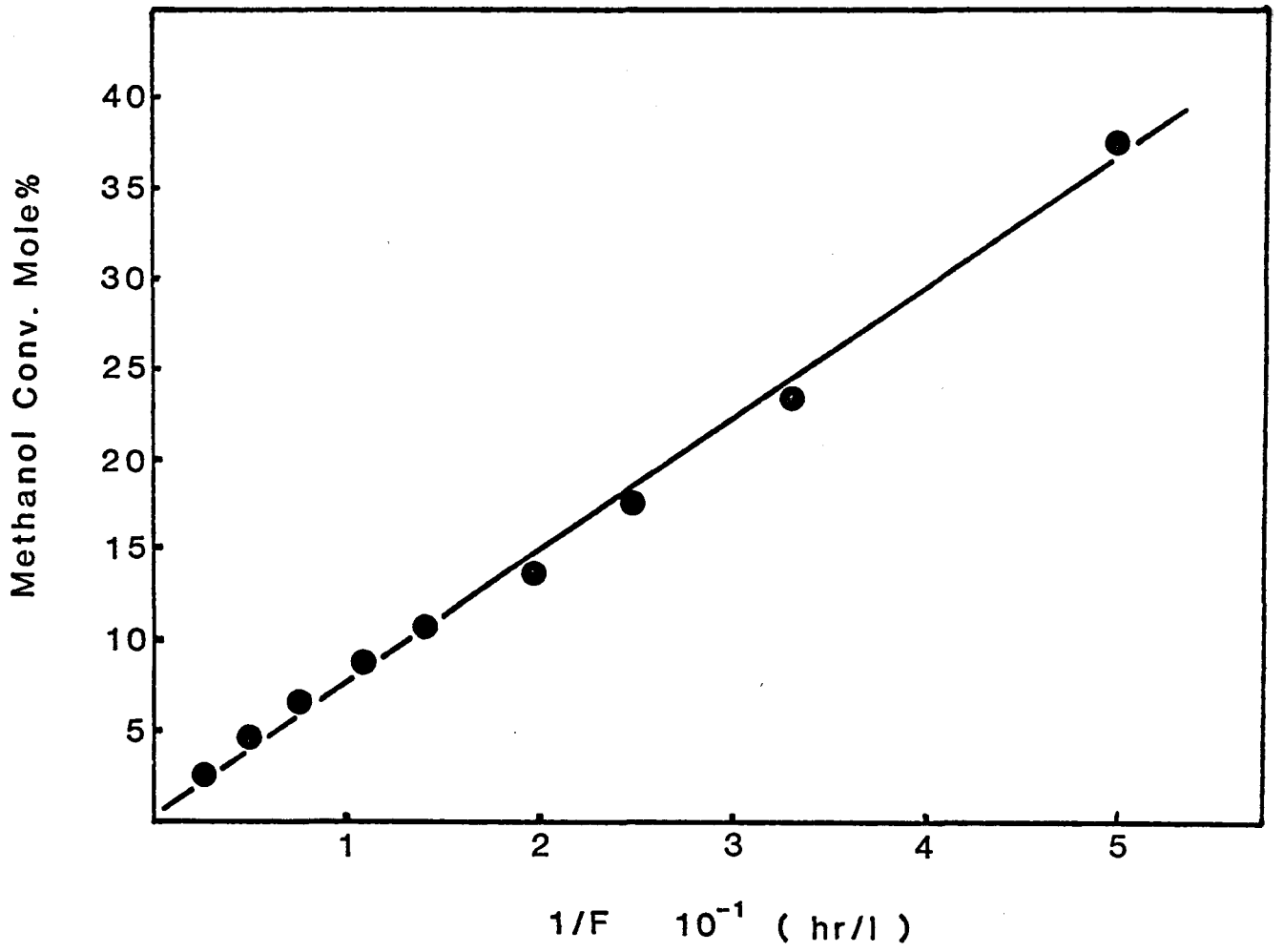

Figure 4.

Relationship between the surface areas of the Cs calcined-doped catalysts before and after testing (Note: surface areas before testing were measured after doping and before reduction)

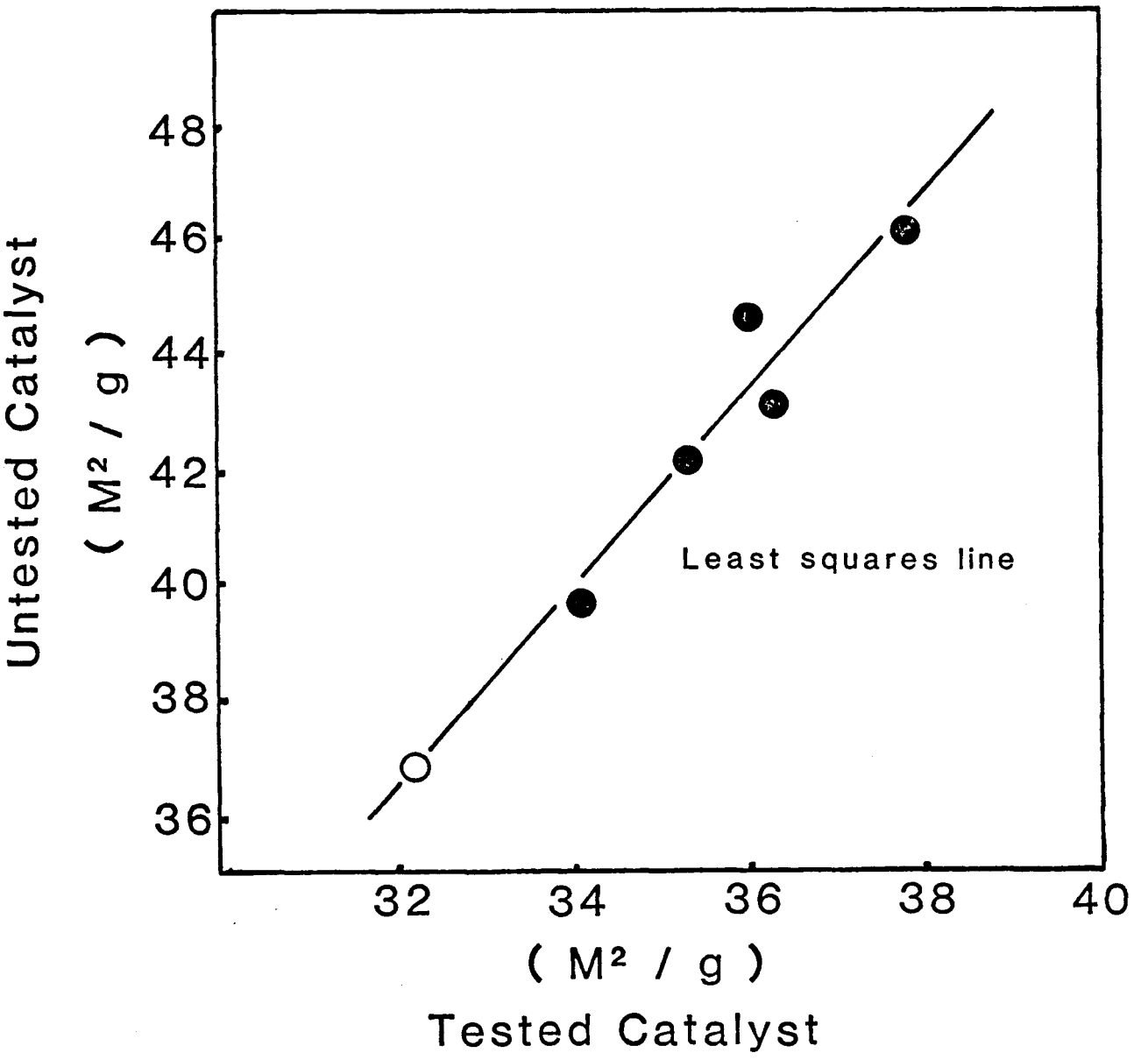

Figure 5.

XPS spectrum of a tested 0.4 mol% Cs calcined-doped catalyst showing the Cu, Zn and Cs photoelectron lines.

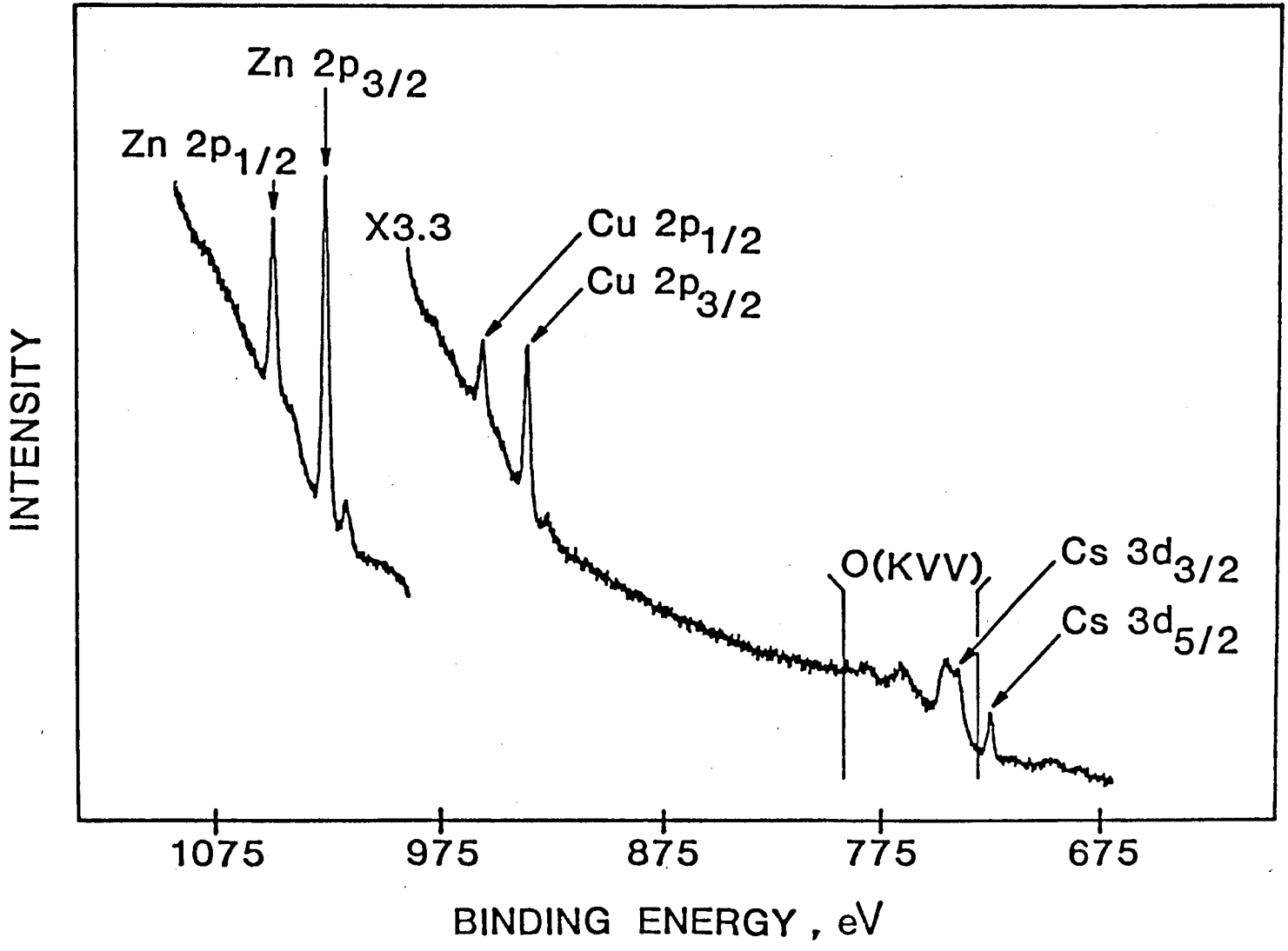

TABLE 1

Particle Dimensions of ZnO and Cu and BET Surface Areas of Calcined-Doped Catalysts

Catalyst (mol%) Cs/Cu/Zn	Dimension (nm)[a] ZnO	Cu	Surface Area (m^2/g) Untested	Tested
0/30/70	13.3	9.3	41.0	37.8
0.15/30/70	13.9	9.0	46.1	37.8
0.30/30/70	13.9	9.3	43.1	36.3
0.40/30/70	13.8	9.0	44.6	36.0
1.00/30/70	13.8	10.3	42.1	35.3
1.00/30/70	14.4	9.9	36.8	32.3[b]
2.00/30/70	15.5	12.2	39.6	34.1

[a] Particle Dimensions of tested catalysts

[b] Surface Area of tested Cs/Cu/Zn = 1/30/70 mol% catalyst extrapolated from Figure 4.

oxidation was unknown as a result of air exposure, and thus could not be accurately quantified. The variance between the measured intensity ratio of Cs to Zn and those calculated, assuming various Cs thickness and location (over Cu or ZnO), are given in Table 2, where n equals the number of Cs monolayer repeat distances perpendicular to the catalyst surface and represents the degree of Cs agglomeration. The monolayer thickness was taken as the sum of the Cs and oxygen ion diameters. In the case with Cs over the ZnO phase, the variance is a minimum for the n=2 calculation. The match is a result of the measured intensity being 13% less than that predicted for a monolayer.

TABLE 2a

X-Ray Photoelectron Data of Calcined-Doped Tested Catalysts

Catalyst (mol%) Cs/Cu/Zn	I_{Cs}/I_{Zn} measured[a]
0.15/30/70	0.00596
0.30/30/70	0.0117
0.40/30/70	0.0217
1.0/30/70	0.0613
1.0/30/70	0.0762
2.0/30/70	0.1692

TABLE 2b

X-Ray Photoelectron Analysis of Calcined-Doped Tested Catalysts

	Variance to measured Intensities[b]			
Model	n=1	n=2	n=3	n=4
Cs over Cu	0.0252	0.0330	0.0392	0.0447
Cs over ZnO	0.0117	0.0018	0.0119	0.0205

[a] Integrated intensity ratio of the Cs $3d_{5/2}$ and Zn $2p_{3/2}$ photoelectron lines.

[b] n equals the number of Cs monolayers perpendicular to the catalyst surface.

In the case of Cs over the Cu phase the best match between the experimental and calculated intensities occurs with n=1, as shown in Table 2. Comparison of the variances of the Cs over Cu model to the Cs over the ZnO shows that the latter model better represents the Cs distribution over the catalyst surface. A plot of the measured intensities and the best matched calculated values for the two models is given in Figure 6. Within the experimental uncertainty, Cs is dispersed over the ZnO. Additionally, the agreement between the measured and calculated values, particularly at the higher Cs concentrations, shows that the degree of Cs dispersion was independent of the bulk Cs concentration.

Quantitative surface analysis of the untested doped samples was not possible because the chemical state and morphology of the Cu and Zn surface components were unknown. This was indicated by the XPS intensity changes of Cu and Zn as a function of Cs concentration, see Table 3. The relative intensity ratio of Cu to Zn decreased with increasing Cs, with the 2.0 mol% sample having a ratio closest to that of the undoped sample.

The relative intensity ratios of Cs to Zn and Cu, normalized to the 0.15 mol% Cs sample and corrected for the respective surface areas (Table 1), are compared to the values expected for a linear increase with Cs concentration in Figure 7. The non-linear relationship for both Cu and Zn indicate that the Cs is "covered" to a larger extent at the lower Cs concentrations. This result is different from the linear relationship observed in the tested catalysts, which indicates that rearrangement of the catalyst surface occurred during catalyst activation.

Figure 6.

Comparison of the measured XPS intensity ratios of Cs and Zn with those predicted for two separate models based on Cs location and mode of surface coverage. n equals the number of Cs-O layers perpendicular to the catalyst surface.

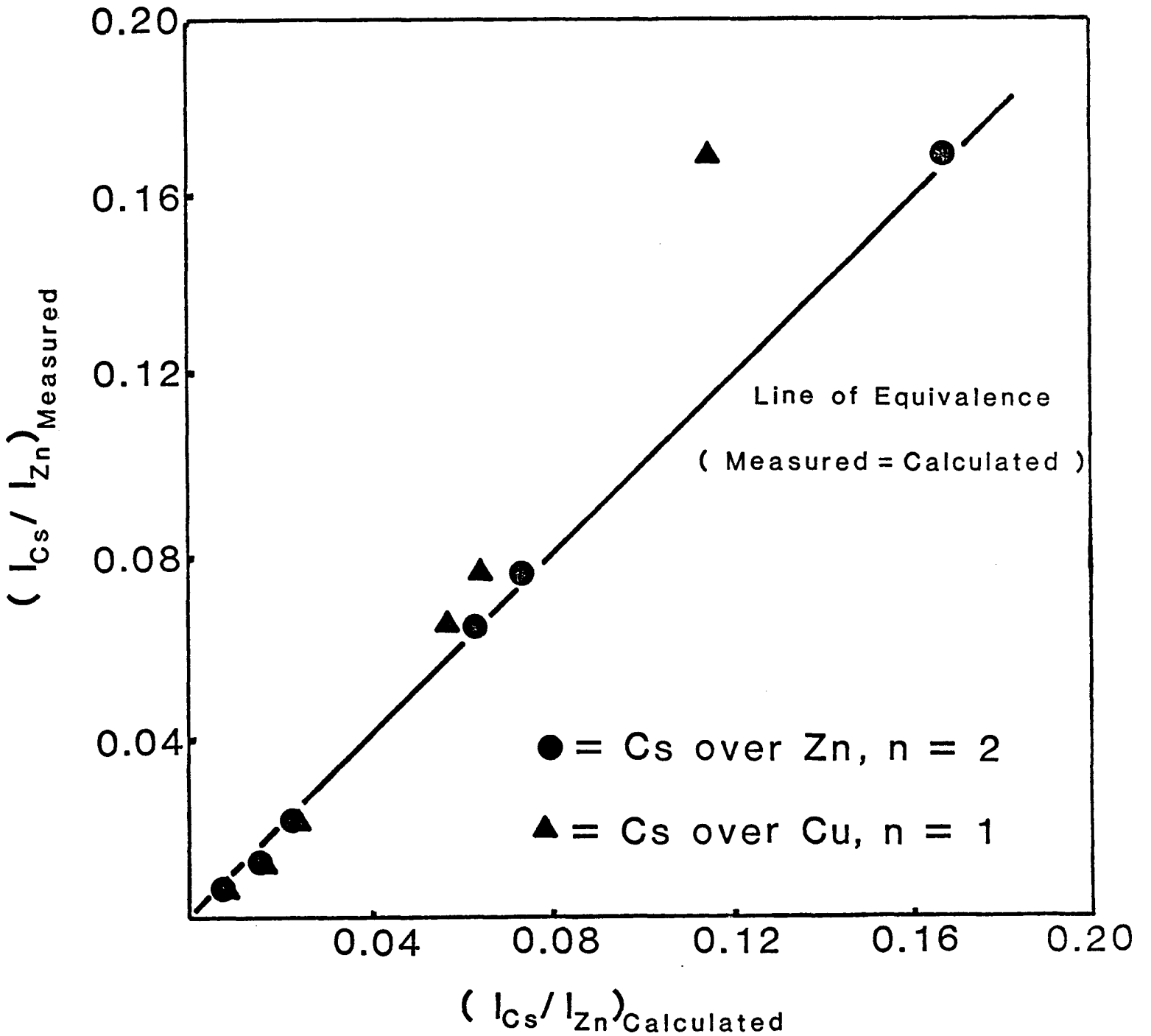

Figure 7.

Plot of the predicted intensity ratio of Cs to Zn and Cu, normalized to the 0.15 mol% Cs sample, vs that observed experimentally for the untested calcined-doped samples. (Note: the differences in surface area were taken into account).

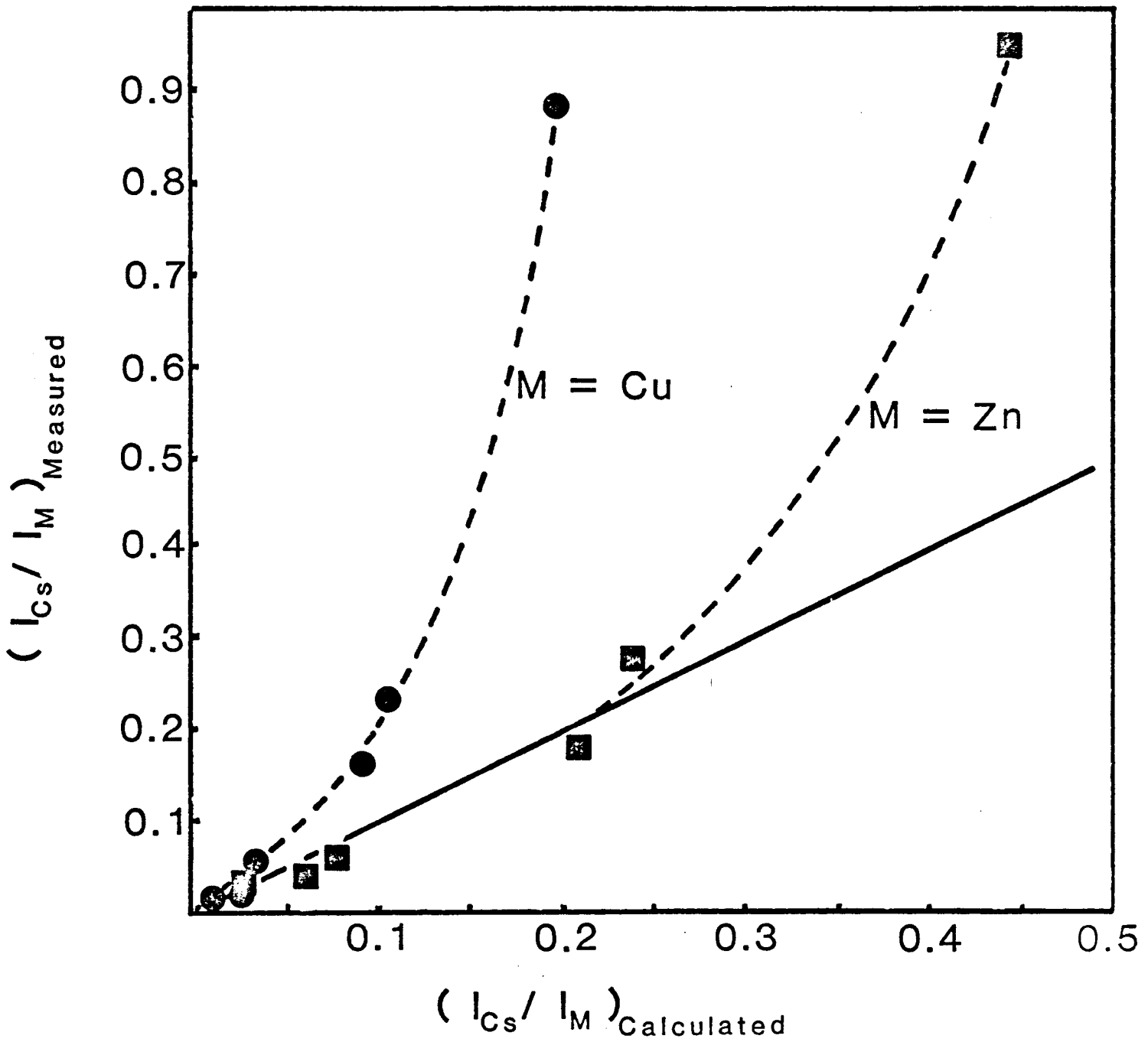

It was further found that the synthesis rates could be correlated to the surface Cs coverage as determined by XPS. However, before this can be done a reinterpretation of the surface analysis results of Figure 6 and Table 2b is necessary so as to define the true Cs coverage. Comparison of the measured and theoretical XPS intensities in the calcined-doped tested samples showed that Cs dispersed over ZnO best represented the catalyst surface. The intensity ratios of Cs to Zn were approximately 13% less than that expected for a Cs monolayer.

TABLE 3

X-Ray Photoelectron Data of the Calcined-Doped Untested Catalysts

Catalyst (mol%) Cs/Cu/Zn	Relative Intensity[a] Zn	Cu	Cs
0.15/30/70	100	44.8	0.457
0.30/30/70	100	42.5	0.657
0.40/30/70	100	21.8	0.972
1.00/30/70	100	22.9	2.95
1.00/30/70	100	23.8	4.45
2.00/30/70	100	21.5	15.30
0/30/70	100	18.5	0

[a] Integrated intensities of the Zn $2p_{3/2}$, Cu $2p_{3/2}$, and Cs $3d_{5/2}$ photoelectron line.

The 13% intensity decrease was consistent for all Cs concentrations, and therefore the cause of the decrease was systematic, and could have been produced by one of the following: 1) the presence of a Cs bilayer approximately 1.2 nm thick, as discussed in the Appendix; 2) an additional component preferentially covering the Cs monolayer, approximately 0.27 nm thick, perhaps such as adsorbed CO_2, CO or strongly attached H_2O or; 3) a systematic error in the ancillary data, which could include uncertainties in the escape depth, monolayer thickness of Cs or Zn, or in the photoionization cross section. An increase in the carbon or oxygen XPS intensity was not observed, which rules out the presence of a contamination overlayer. It is also unlikely that a consistently uniform bilayer would form independent of the bulk Cs concentration. Further agglomeration would be expected at the higher Cs concentrations, but this was not observed. It is more reasonable that a small systematic error arose from the ancillary data, and that the Cs is atomically dispersed as a monolayer. Consequently, the following analysis will be carried out on the premise that Cs is atomically dispersed. It is anticipated that this issue will be resolved in the near future by the use of standards.

Combining the synthesis rate, catalyst surface area, and concentration of atomically dispersed Cs, the specific activities per m^2cat were determined, and are shown in Figure 8. Promotion by Cs increased the specific activities by over 2 for methanol, 5 for ethanol, and 7 for methyl-formate. The specific activity per Cs atom is given by the slope of the curves, which are markedly different for each product in two ways - the absolute quantity and the range in Cs concentration in which the slope is constant. The latter observation can be used to approximate the Cs coverage for which the

Figure 8.

Plot of the specific activities of the calcined-doped catalysts, expressed as yields per m^2 of catalyst for methanol, methyl formate and ethanol as a function of Cs atom concentration per m^2 of catalyst (calculated from XPS data). (Note: reaction conditions were the same as for Figures 1 and 2).

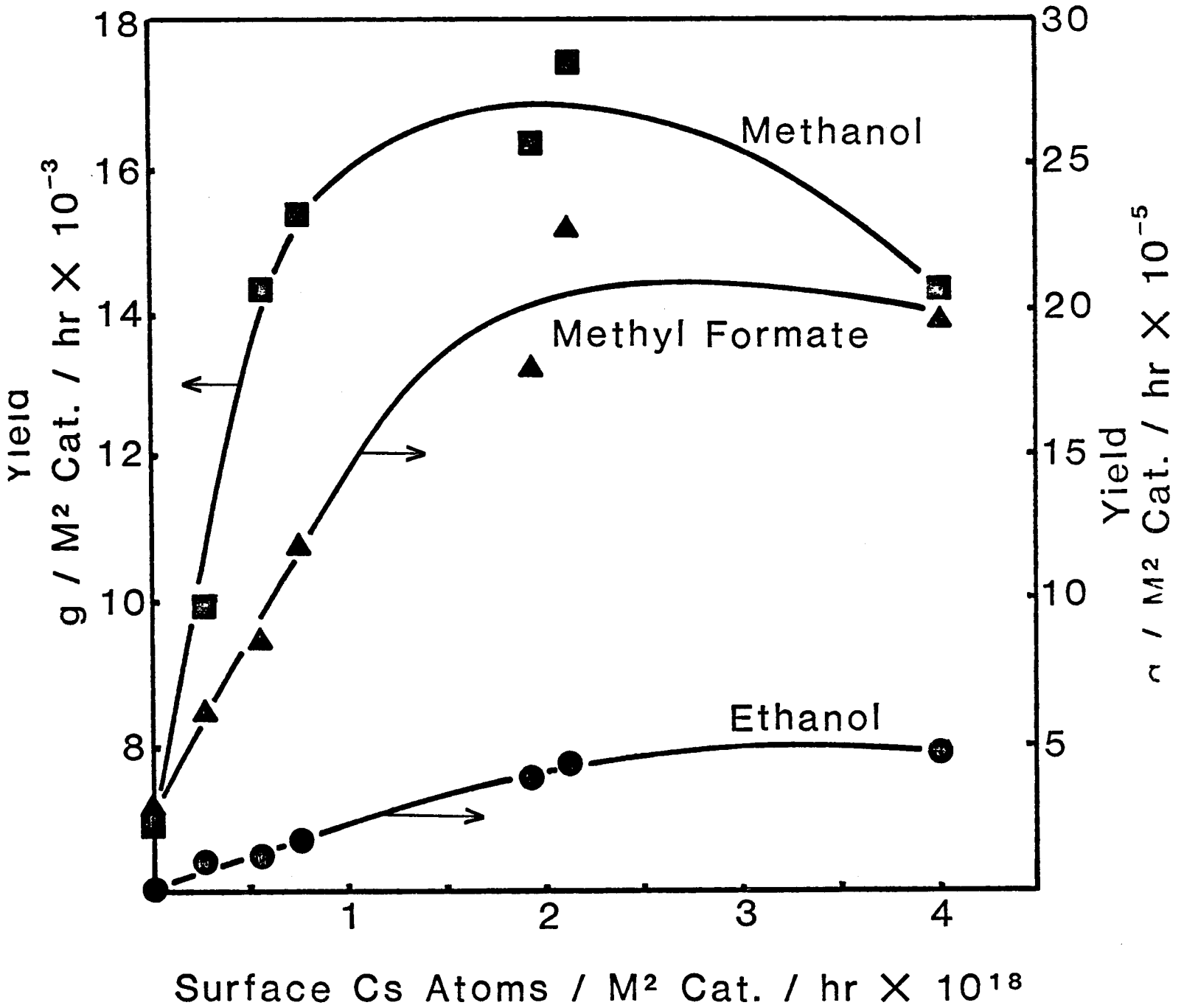

maximum promotion effect occurs.

The Cs coverage is given in terms of the ZnO surface area, as this was shown to be where the Cs resides in the Cu/ZnO system. The coverage is calculated from the relation, $N_{Cs}S_{Cs}/S_{ZnO}$, where N_{Cs} equals the number of Cs ions, S_{ZnO} the ZnO surface area (see Appendix for calculation), and S_{Cs} the Cs ion effective surface area taken as $\pi(\text{radius})^2$ with the ionic radii of Cs, 0.167 nm (2). To aid in comparing the surface coverages, the specific activities were normalized and plotted versus the Cs coverages, and the results are shown in Figure 9. The maximum promotion effect occurred with coverages up to θ_{Co} = 0.12 for methanol, θ_{Co} = 0.19 for methyl-formate and θ_{Cs} = 0.31 for ethanol.

The long term stability of one of the catalysts (0.4 mol%) Cs/Cu/ZnO, calcined-doped) was examined under higher alcohol conditions, the results being summarized in Table 4. It is evident that after 300 hr of testing the catalyst had lost about 35% of its initial activity. The higher alcohol synthesis testing conditions are given in Table 4, and the degree of deactivation was measured by changing the reaction condition to T = 250°C, H_2/CO = 70/30 and CO + H_2 feed = 15 l/hr and comparing the activity with that initially observed under steady state conditions. This was done since previous studies showed that under these conditions the catalytic activity could be related to the surface area and Cs coverage. After removing the catalyst from the reactor it was found that the surface area had decreased from 36.0 to 13.72 m^2/g.

Figure 9.

Plot of specific activities, vs the surface Cs coverage over ZnO, normalized for constant initial slope, for ethanol, methyl formate and methanol.

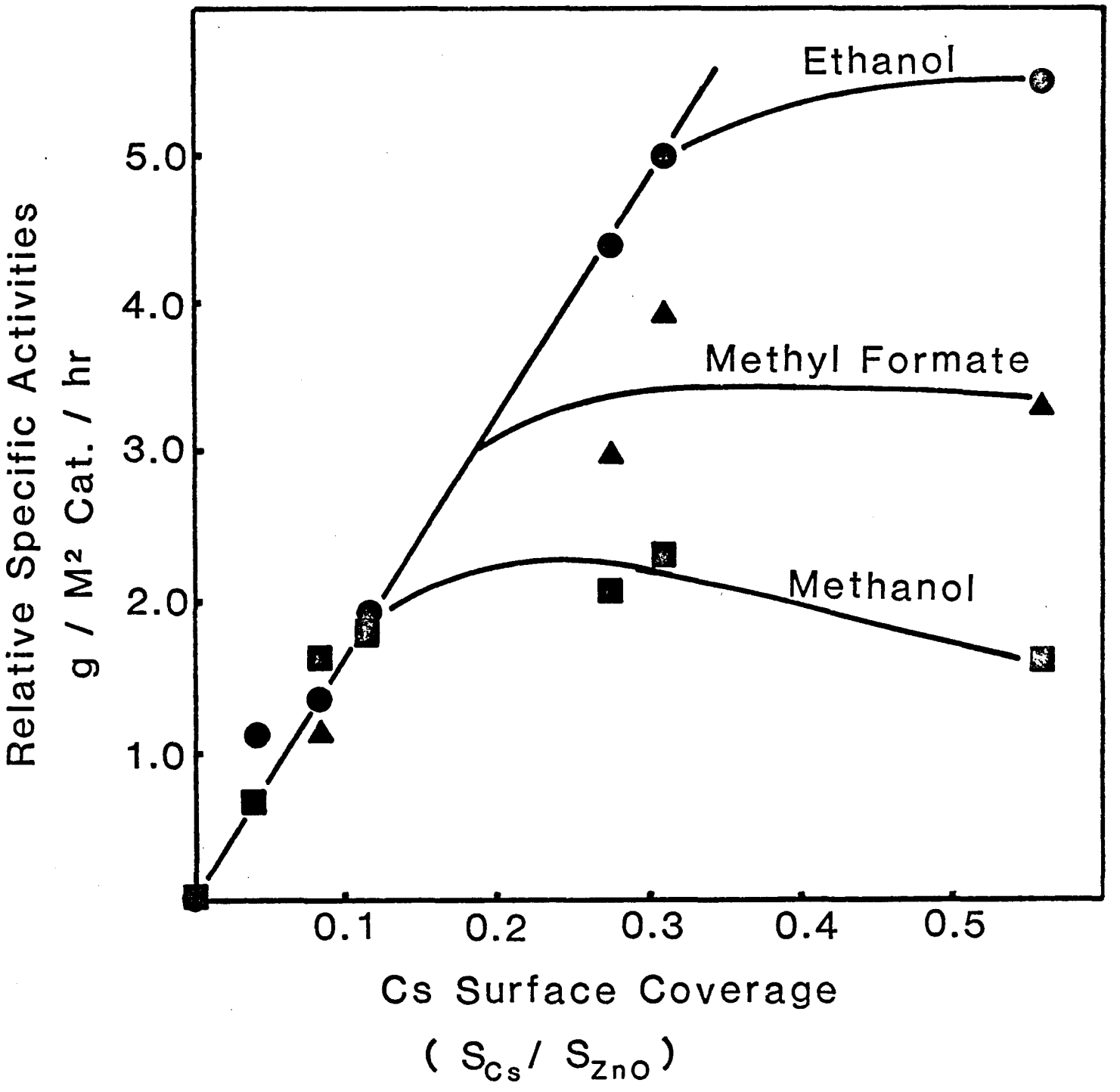

TABLE 4

Effect on activity* at 250°C after testing a 2.8 g portion of a 0.4 mol% Cs/Cu/ZnO catalyst for 300 hr under higher alcohol synthesis conditions, where testing conditions were: T = 310°C, P = 75 atm, H_2/CO = 0.45 and CO + H_2 feed rate = 8 ℓ/hr.

Time of Testing	Mol% conversion of CO*
Before Higher Alcohol Testing	24.57
After Testing	16.0

* Activities compared at T = 250°C, P = 75 atm, H_2/CO = 2.33 and Feed = CO + H_2 = 15 ℓ/hr.

Future Work

Work now in progress and future work will concentrate on the preparation of a stable Cs/Cu/Zn/Al catalyst. As in the case of the Cs/Cu/ZnO catalyst the preparation will involve the synthesis of a single morphology precursor followed by doping with Cs. In the case of Cu/Zn/Al the precursor of choice is hydrotalcite HC, $(Cu,Zn)_6Al_2CO_3\cdot(OH)_{16}\cdot 4H_2O$. This precursor compound has the following desirable properties:

(i) The HC precursor has been shown to be a suitable starting material for making an active methanol synthesis catalyst (10,11).

(ii) Decomposition of HC leads to Cu/Zn/Al platelets with a very high dispersion of the elements Cu, Zn and Al, a feature which is considered very important in maintaining high catalyst stability.

(iii) Methanol synthesis promotion by Cs over Cu/Zn/Al catalysts in the absence of CO_2 or H_2O has previously been demonstrated in these laboratories.

(iv) The HC precursor is readily characterized by XRD, thus allowing preparation reproducibility to be easily verified.

(v) Because of the unique structure of HC, its chemical composition can be varied over a wide range:

$$HC = (Cu_xZn_{1-x})_6Al_2(CO_3)(OH)_{16}\cdot 4H_2O \ .$$

$0 \leq \frac{Cu}{Cu+Zn} \leq 0.5$ and $0.24 \leq \frac{Al}{Al+M^{n+}} \leq 0.31$ while still maintaining its integrity.

Pure HC compounds have been prepared by coprecipitation at constant pH (10,12) and this is the method of choice. Relatization of a continuous-fixed pH-coprecipitation can be accomplished by the controlled mixing of Na_2CO_3 and the salts of Cu, Zn and Al. An apparatus has been especially built for this purpose, equipped with high precision pumps to supply the salts at fixed rates so that a constant pH is maintained (c.f. Figure 10). As with the Cs/Cu/ZnO catalysts, the aluminum-containing testing and untested catalysts will be characterized by the full range of techniques available at Lehigh including XPS, TEM, XRD U.V. reflectance/IR and BET.

Figure 10

Apparatus for Continuous-Fixed pH-Coprecipitation

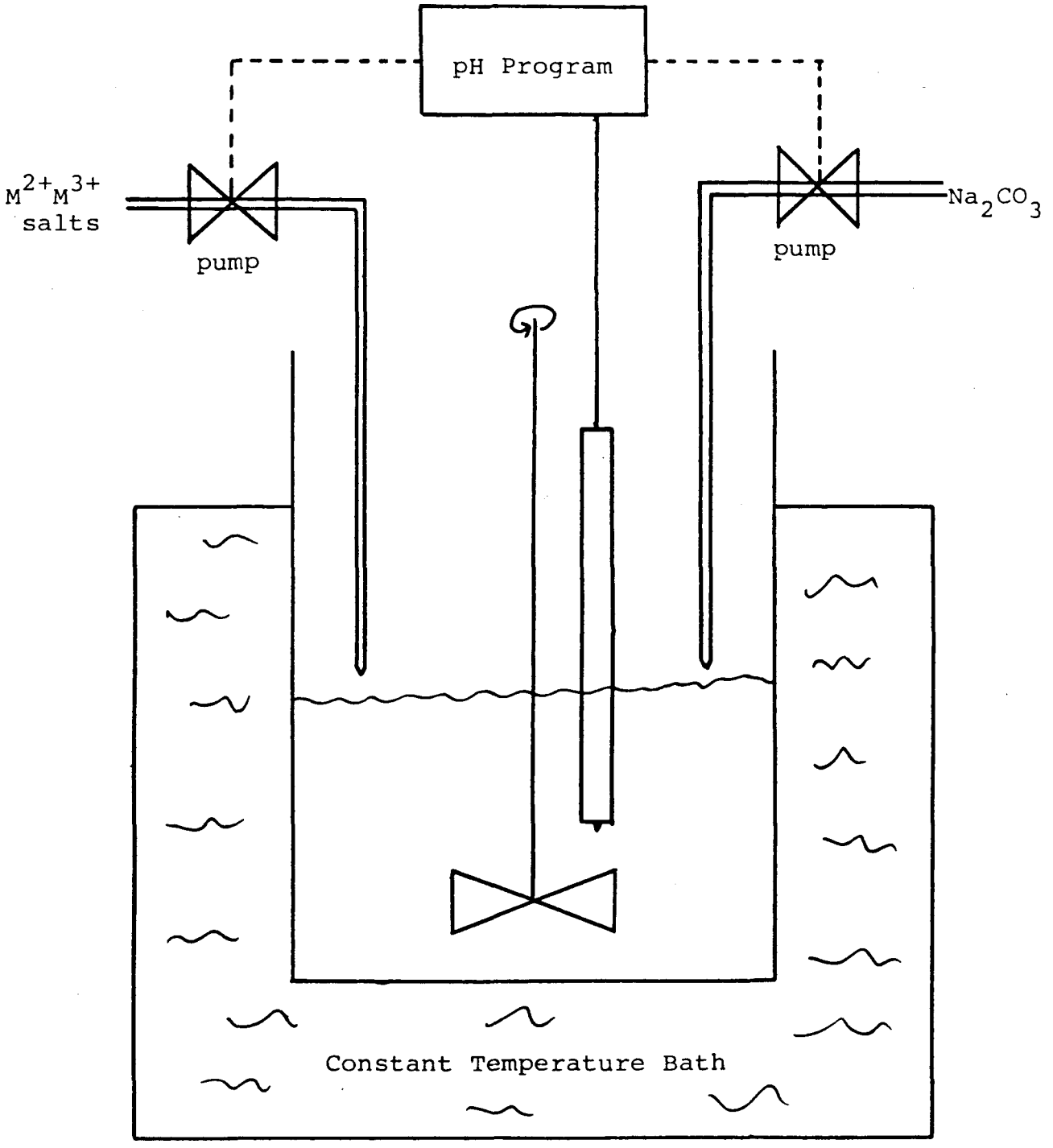

B. Analytical Gas Chromatography of Catalytically Generated Synthetic Alcohol Fuels

The application of capillary gas chromatography as an analytical procedure for the characterization of products generated from the higher alcohol synthesis reactions is the subject of this report. Separations of C_1 through C_4 products have primarily been achieved by using a 6' by $\frac{1}{8}$" diameter column packed with Porapak Q. The instrument used was a Hewlett-Packard Model 5730A gas chromatograph equipped with an automatic sampling valve and a thermal conductivity detector. Idenitifcation of the components was based on the retention time of the unknown compounds, and quantitative information was obtained with a Hewlett-Packard Model 3388A integrator coupled to the GC. Complications arose when attempts were made at separating the higher alcohol synthesis products, e.g. the C_5, C_6, and C_7 products, with the Porapak Q column. Peaks were observed to broaden and overlap in this range for all conditions. Therefore, to achieve separation of the C_5 and C_6 products appearing in small amounts, possibly trace quantities, three different capillary columns varying in degree of polarity were tested to see which would give optimum separation and resolution of the products. The three columns tested were [A] 30 m long by 0.32 mm I.D. 50% phenyl methyl silicone capillary column, [B] 26 m long by 0.33 mm I.D. Carbowax capillary column, and [C] a 60 m long by 0.75 mm I.D. wide bore bonded methyl silicone capillary column. The columns were separately tested and used in a Hewlett-Packard Model 5880A gas chromatograph with a flame ionization detector. Also coupled to the GC was a Hewlett-Packard 5880A series GC terminal integrator providing quantitative information by deter-

mining the areas under the peaks in the chromatograph.

Component identification was accomplished by using a retention index system based on the retention times of pure standards. To optimize peak resolution the following parameters were studied: column flow rate, oven temperature programming, and sample dilution in various solvents. The figures that follow show the results obtained with each column and the influence of varying the above parameters.

Results

The selection of the appropriate capillary column for the total analysis of higher alcohol synthesis products began by first looking at the chromatographs produced by the Porapak Q 6' column. In our previous research, catalysts were studied with the primary emphasis on the methanol regime, and Figure I shows the separation by the Porapak Q column of the reaction products for methanol synthesis. The analysis became more complex when studying the products of the alkali-doped catalysts as seen in Figure II, where it is seen that the C_1 through C_4 products can be resolved on the Porapak Q column without much broadening or peak-overlapping. The separation problem arose when products with a higher carbon number were added to the feed gas to derive mechanistic data. Figure III shows the chromatograph of higher alcohol synthesis products from synthesis gas with 2-methyl-1-propanol also being pumped with the feed. The peaks became broad and overlapped to a large extent at retention times longer than that for the C_4 product. When the same product mixture was analyzed on the wide bore methyl silicone capillary column shown in Figure IV-B, it was

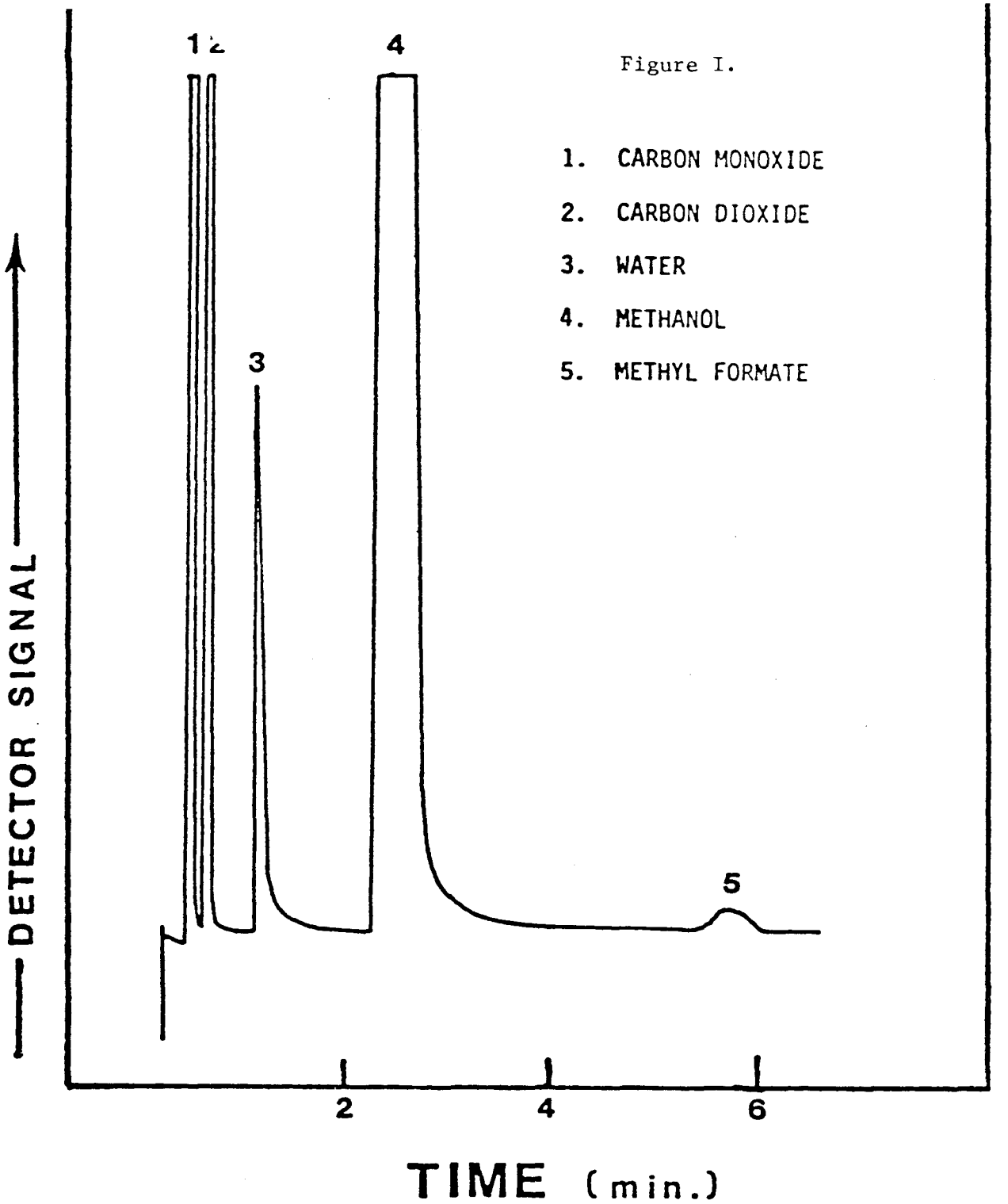

Figure I.

GAS CHROMATOGRAPH OF THE REACTOR PRODUCTS FOR METHANOL SYNTHESIS FROM SYNTHESIS GAS (H_2/CO = 2.33) AT 15 l/hr, 288 ^{o}C, 75 ATM.
COLUMN: POROPAK Q ISOTHERMAL RUN AT 90 ^{o}C.

Figure II.

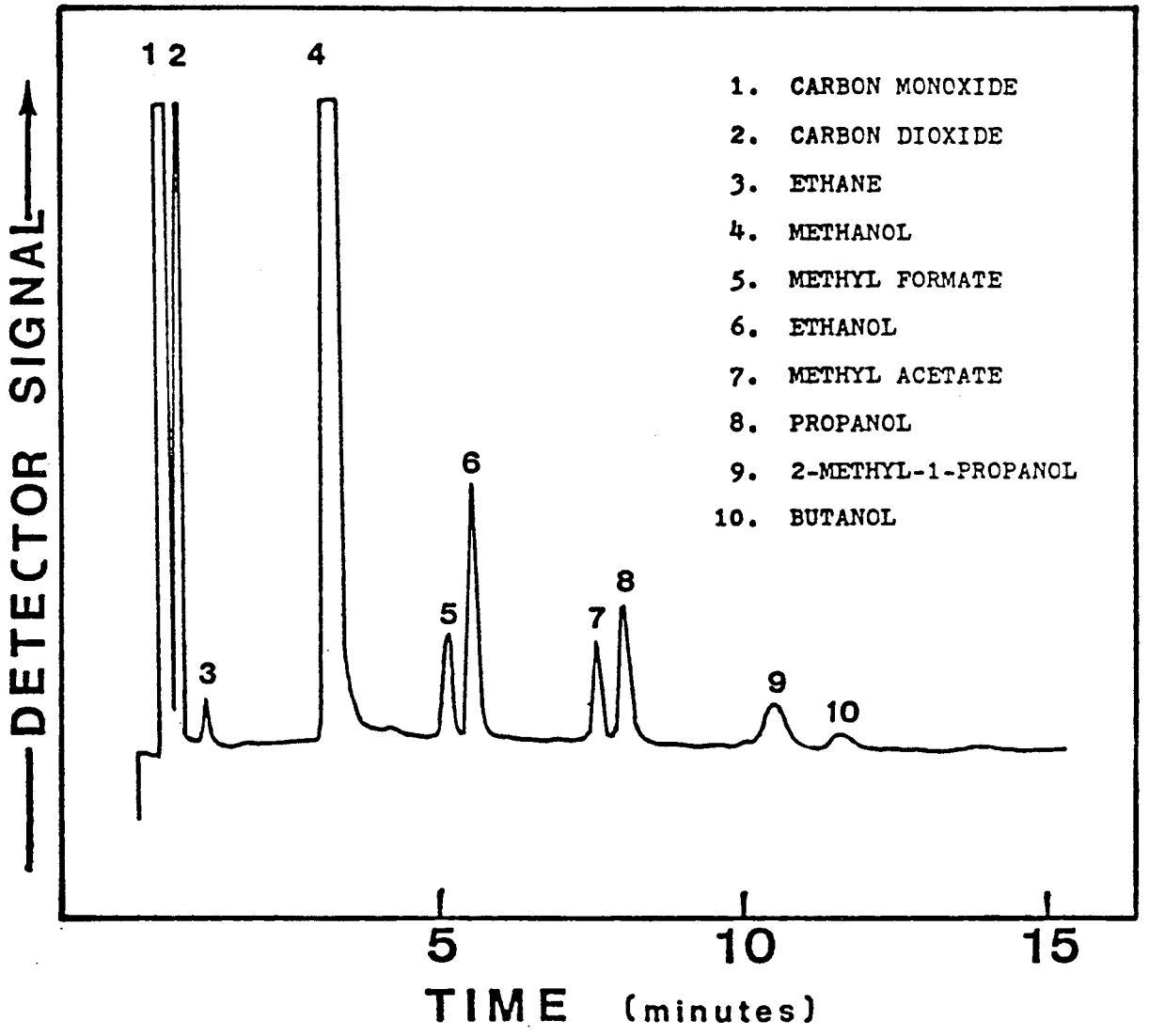

Gas chromatograph of the reactor products for higher alcohol synthesis from synthesis gas (H_2/CO = 0.45) at 8 liters/hr. 288°C, 75 atm. over Cu/ZnO/ KOH (= 30/70/0.4) catalyst.

Column: Poropak Q

Temperature Program: Hold 2 min. at 90°C, then to 200 C at 16°C/min.

Figure III.

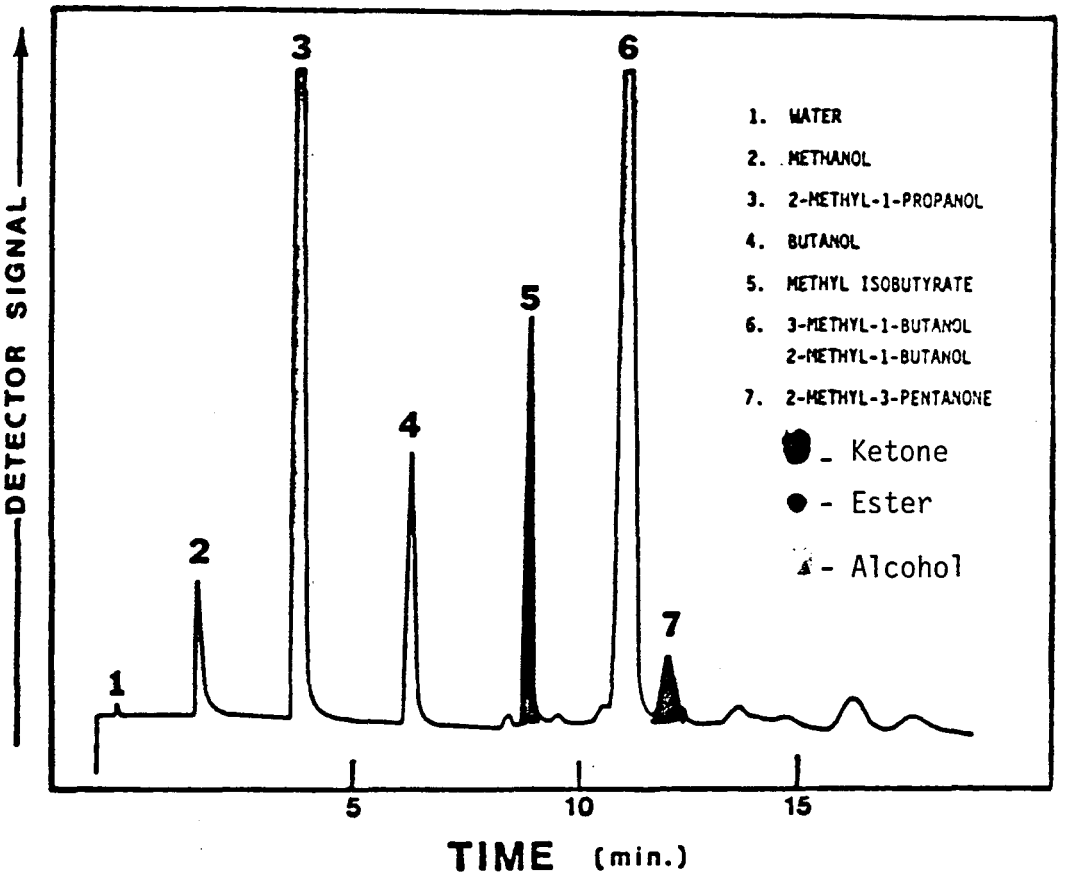

Gas chromatograph of the reactor products for higher alcohol synthesis from synthesis gas (H_2/CO = 0.45) at 8 ℓ/hr, 309°C, 75 atm, and pumping 2-methyl-1-propanol at 5.0 µl/min over the catalyst:

Cu/Zn/Cs Theoretical Metal Molar Ratio = 30/70/0.4
Doped with CsOOCH after Calcination.

Column: Poropak Q Temperature Program: Hold 2 min at 90°C, then to 200°C at 16°C/min.

Figure IV.

A.

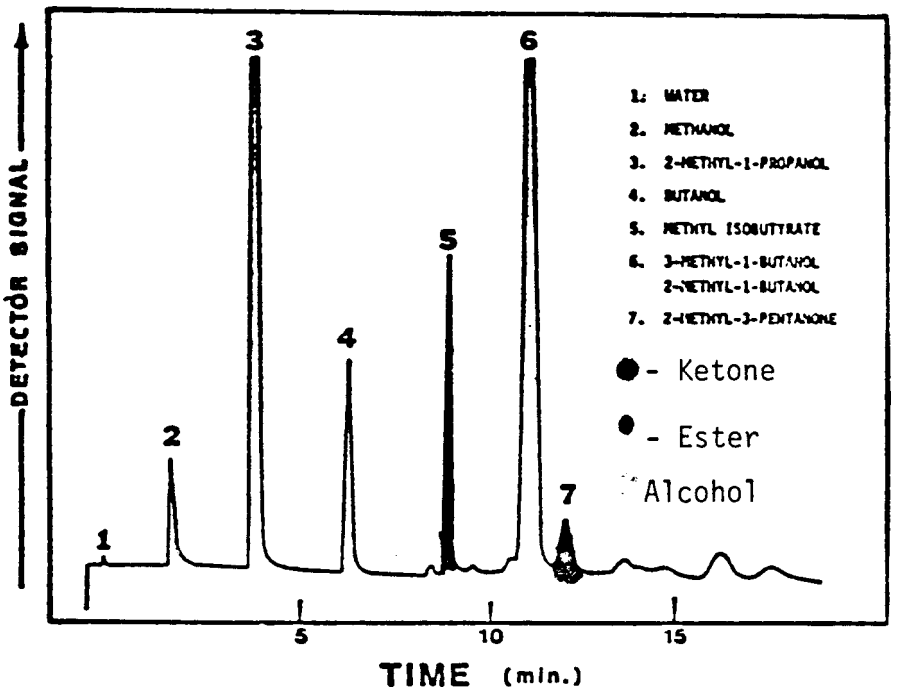
DETECTOR SIGNAL
1
2
3
4
5
6
7
1. WATER
2. METHANOL
3. 2-METHYL-1-PROPANOL
4. BUTANOL
5. METHYL ISOBUTYRATE
6. 3-METHYL-1-BUTANOL
2-METHYL-1-BUTANOL
7. 2-METHYL-3-PENTANONE
- Ketone
- Ester
Alcohol
5
10
15
TIME (min.)

B.

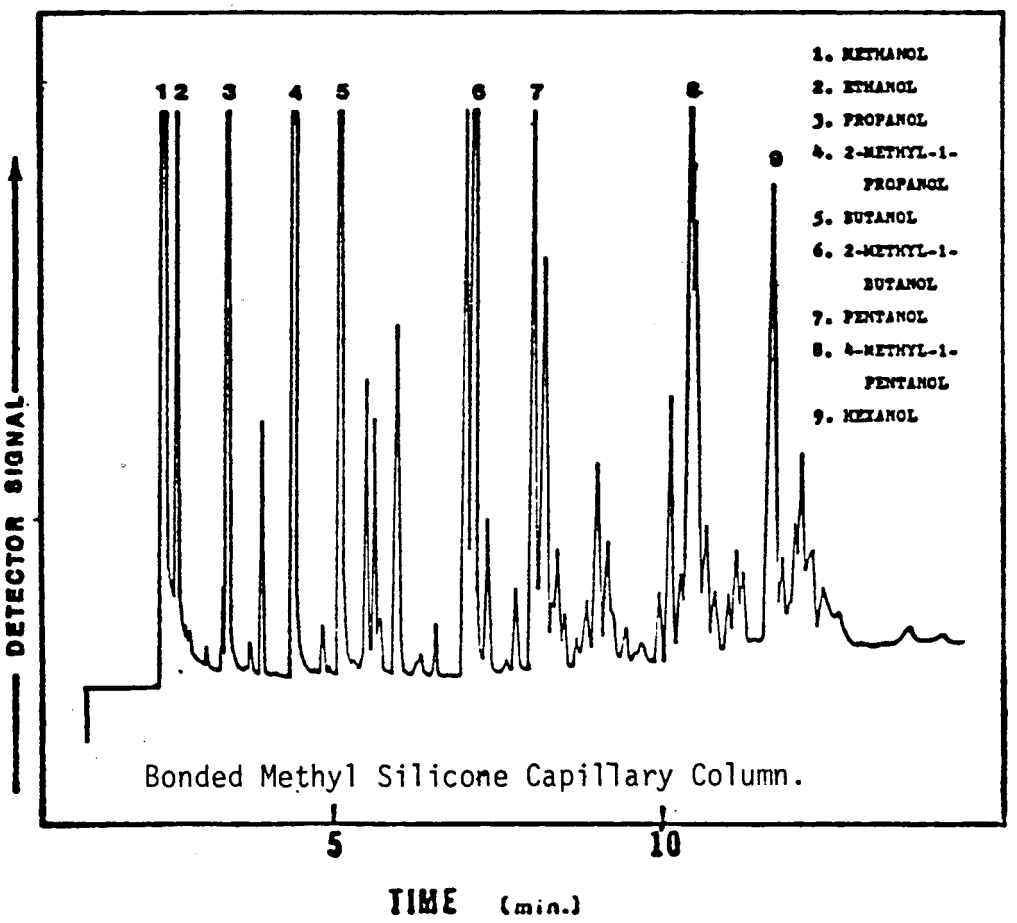
DETECTOR SIGNAL
1 2 3 4 5 6 7 8 9
1. METHANOL
2. ETHANOL
3. PROPANOL
4. 2-METHYL-1-PROPANOL
5. BUTANOL
6. 2-METHYL-1-BUTANOL
7. PENTANOL
8. 4-METHYL-1-PENTANOL
9. HEXANOL
Bonded Methyl Silicone Capillary Column.
5
10
TIME (min.)

clearly seen how poorly the Porapak Q (Figure IV-A) actually resolved the product components. Spiking the Porapak Q packed column led to erroneous identification in the higher alcohol regions because, as Figure IV-B shows, one broad peak in Figure IV-A is actually a combination of a few minor, but vital, products needed for accurate mechanistic studies to be conducted. Unless separation is complete, even the use of a GC/mass spectrometer will give ambiguous identifications.

The chromatogram in Figure IV-B showed that the more efficient separation of the complex higher alcohol product mixture required the smaller diameter and longer column length of a capillary column for complete analyses to be carried out. Three columns having different types of stationary phase coating the capillary column were investigated with a view of providing an optimum separation of all isomers present and also permit analyses of samples with wide concentration ranges. Previously, carbowax columns have been used for the separation of C_1-C_5 alcohols or mixtures of alcohols with other low molecular weight compounds. The carbowax, because of its high polarity, seemed to be a resonable choice for separation of alcohols, esters, aldehydes, and ketones, so a 26m by 0.33 mm I.D. with a 1.4 μm film thickness was tested at various flow rates and different oven temperature programs. The best separation obtained with this column was not good enough to resolve the higher alcohol products, as Figure V demonstrates for the C_5 and C_6 regions. The column examined next was a 50% phenyl methyl methyl silicone capillary column 30 m long by 0.32 mm I.D. with a 1.00 μm film thickness. Various flow rates and a large temperature range were studied, and one of the better separations of the complex higher alcohol mixture is shown in Figure VI. Separation is very poor with peaks eluting from the column too close together with overlap indicating complete identification and quanti-

Figure V.

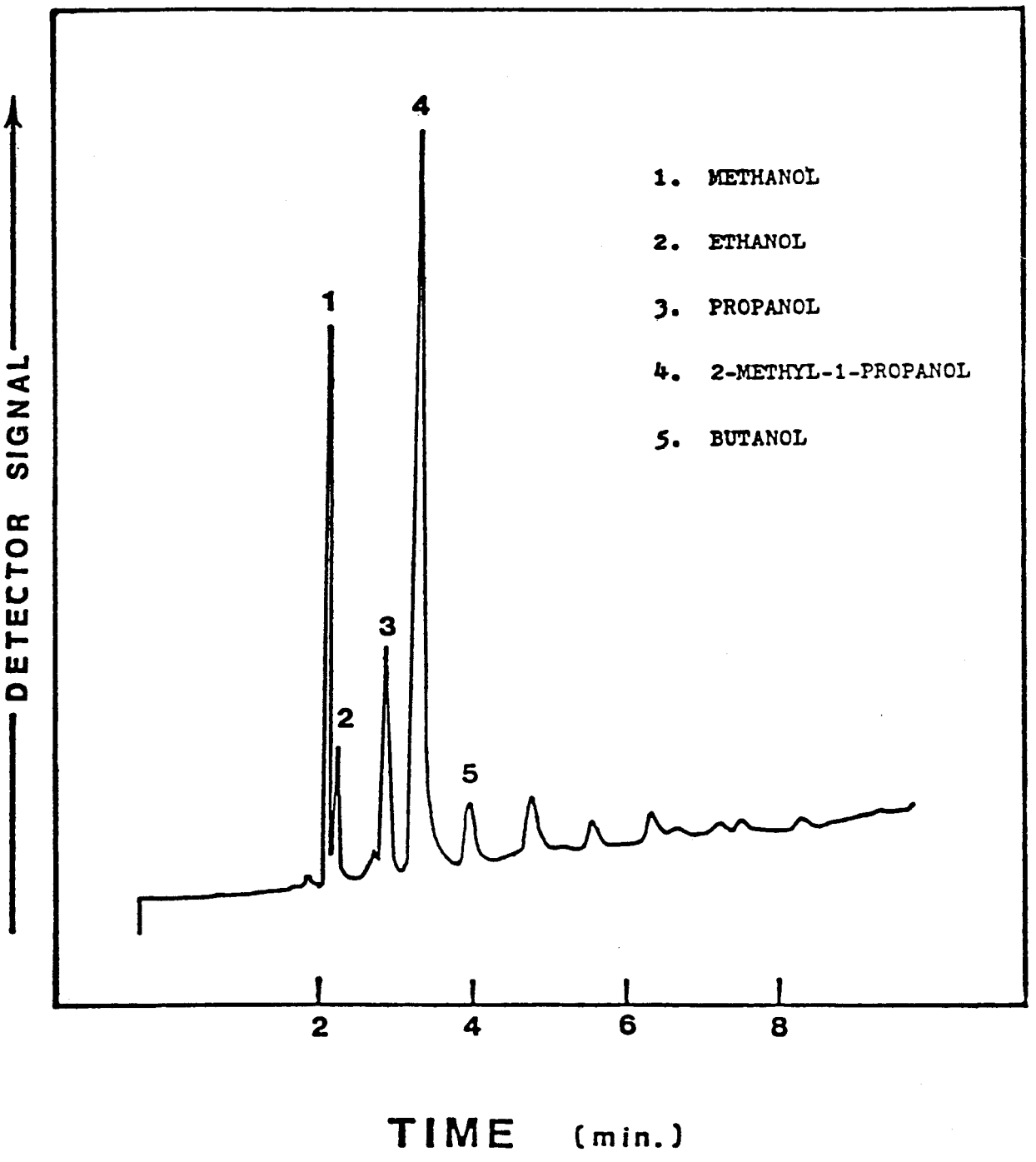

Gas chromatograph of higher alchohol synthesis products over Cu/ZnO/ Cs (=30/70/0.4) catalyst. - CARBOWAX CAPILLARY COLUMN - - POLAR -

Figure VI.

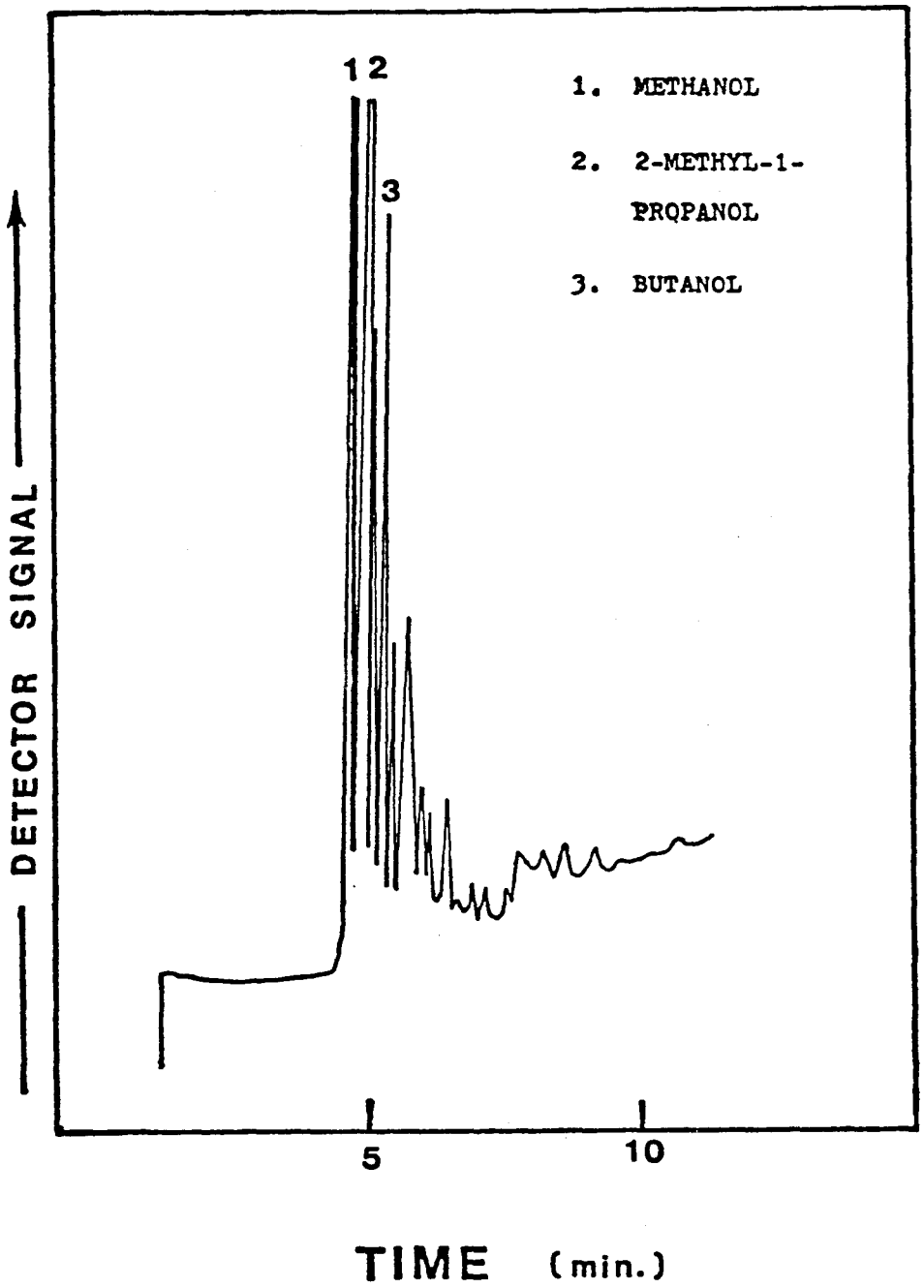

Gas chromatograph of higher alcohol synthesis products over Cu/ZnO/Cs (=30/70/0.4) catalyst.

- 50% PHENYL METHYL SILICONE CAPILLARY COLUMN -

- VERY POLAR -

fication were once again not possible. The last column choice was a bonded methyl silicone wide bore capillary column 60 m long by 0.75 mm I.D.. This column is non-polar and generally permits elution of most samples in order of boiling point and carbon number. This column, when tested under varying flow rates and different temperature programs, provided the desired separation and resolution of the higher alcohol products as seen in Figure IV-B. The C_1 through C_6 regions have been separated as indicated by the labelled peaks in the chromatogram. A complete identification of all the components in the mixture is shown later in the report. The larger diameter of this wide bore methyl silicone column also enabled large sample volumes to be injected and enables on-line analyses to be conducted with the existing set up used for the $\frac{1}{8}$" Porapak Q column with minor alterations.

After selection of the methyl silicone column and an optimum temperature program were found, experiments were carried out to determine if further resolution of the components could be obtained by utilizing different solvents. Pentane and Haptane were compared to the original undiluted higher alcohol sample, and Figure VII shows the sample in both solvents. Pentane seemed to be the better of the two solvents because it eluted before the C_5 region, which prevents a possible overlap of solvent peak with a component as is the case with heptane obscuring 2-pentanol and 3-pentanol. Pentane also enabled separation of components such as 2-methyl-1-butanol and 2-methyl-1-butanol, where heptane only slightly separated these two components with a lot of overlap of the peaks, which made quantification difficult. The same degree of resolution as obtained with the

Figure VII

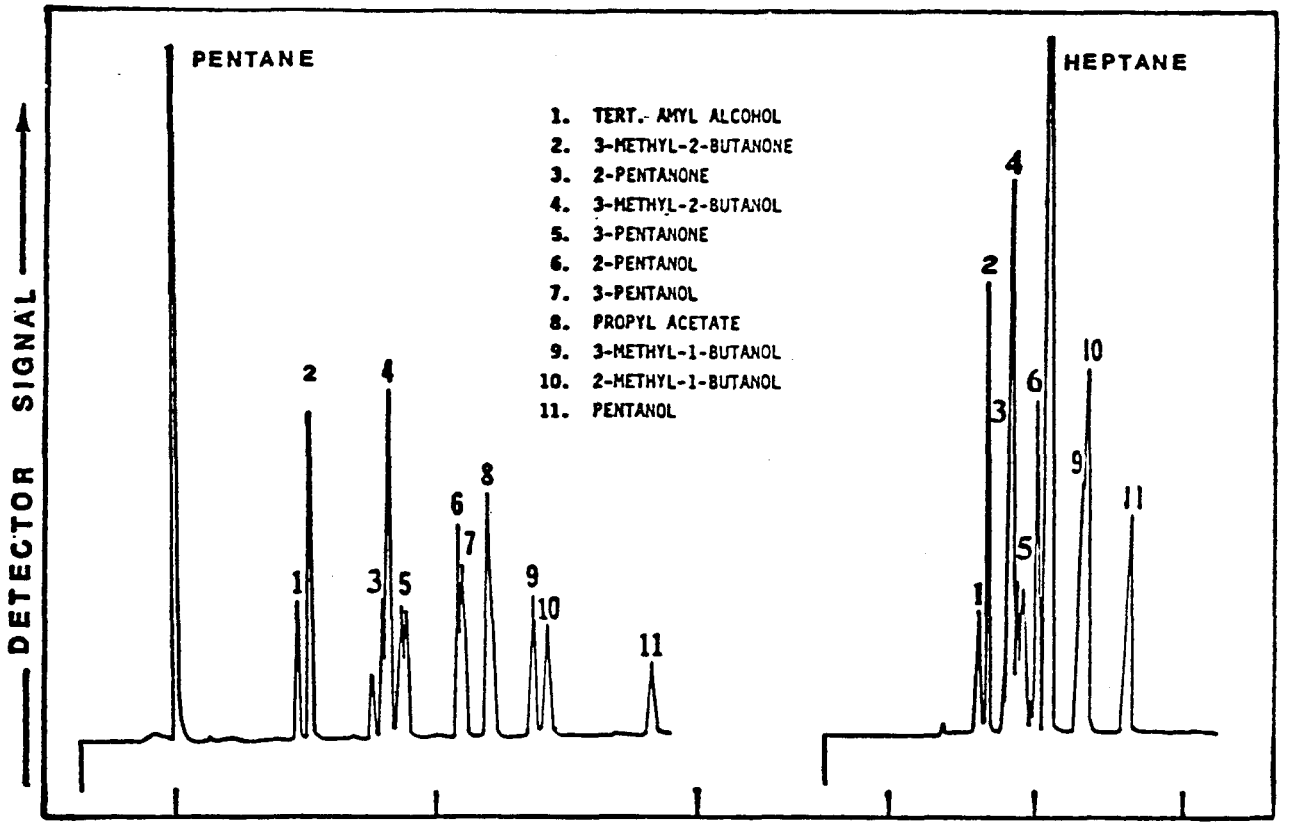

GAS CHROMATOGRAPH OF C_5 ALCOHOLS IN THE SOLVENTS PENTANE AND HEPTANE.

COLUMN: WIDE BORE BONDED METHYL SILICONE CAPILLARY COLUMN.

pentane solvent system was obtained from the pure sample with no solvent added. This may be due to the fact that methanol and a few of the other lower alcohols were present in such large amounts that they could act as solvents for the other components of the mixture. This offered the choice of using pentane as a solvent or simply analyzing the sample undiluted - depending on the complexity of the sample and if on-line analysis were used as opposed to manual injection.

Finally, injection conditions were varied to see if this could improve the chromatographic separation. First a standard was injected with the injection port temperature at 220°C, Figure VIII, and then the same standard was injected with the port temperature at 70°C, Figure IX. The chromatogram of the sample injected at 220°C showed the presence of a few small peaks, which were not present with the "cool on column injection" being used. These peaks may have been caused by fragments of higher molecular weight components that decomposed under the high temperature conditions, or they may be due to molecular species formed by reactions between some of the primary products. Therefore, cooler injection temperatures were chosen to reduce error for quantitative analyses.

Samples were collected over a range of conditions on a standard Cu/Zn/Cs catalyst to see if this capillary column was capable of separating all higher alcohol products at extreme conditions where the most complex product mixtures were produced. Figure X shows the product distribution when the catalytic reactor was operated at 290°C. A sample was also collected at a more severe condition of 209°C and it is seen in Figure XI

Figure VIII

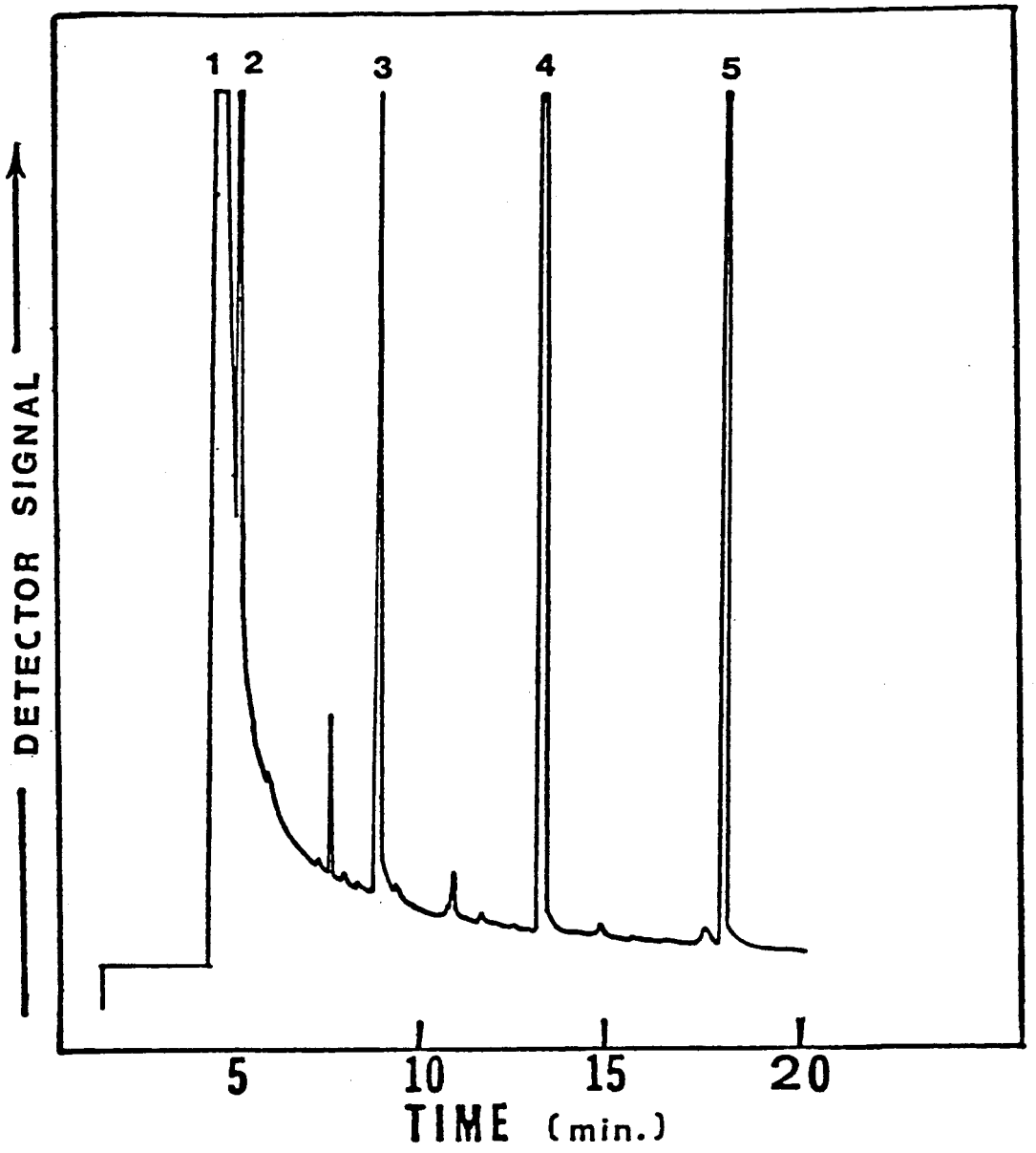

INJECTION AT 220°C.

WIDE BORE BONDED METHYL SILICONE CAPILLARY COLUMN

COMPONENT

1. METHANOL
2. 2-PROPANOL
3. 3-METHYL-2-BUTANOL
4. 2-HEXANOL
5. METHYL CAPROATE

Figure IX

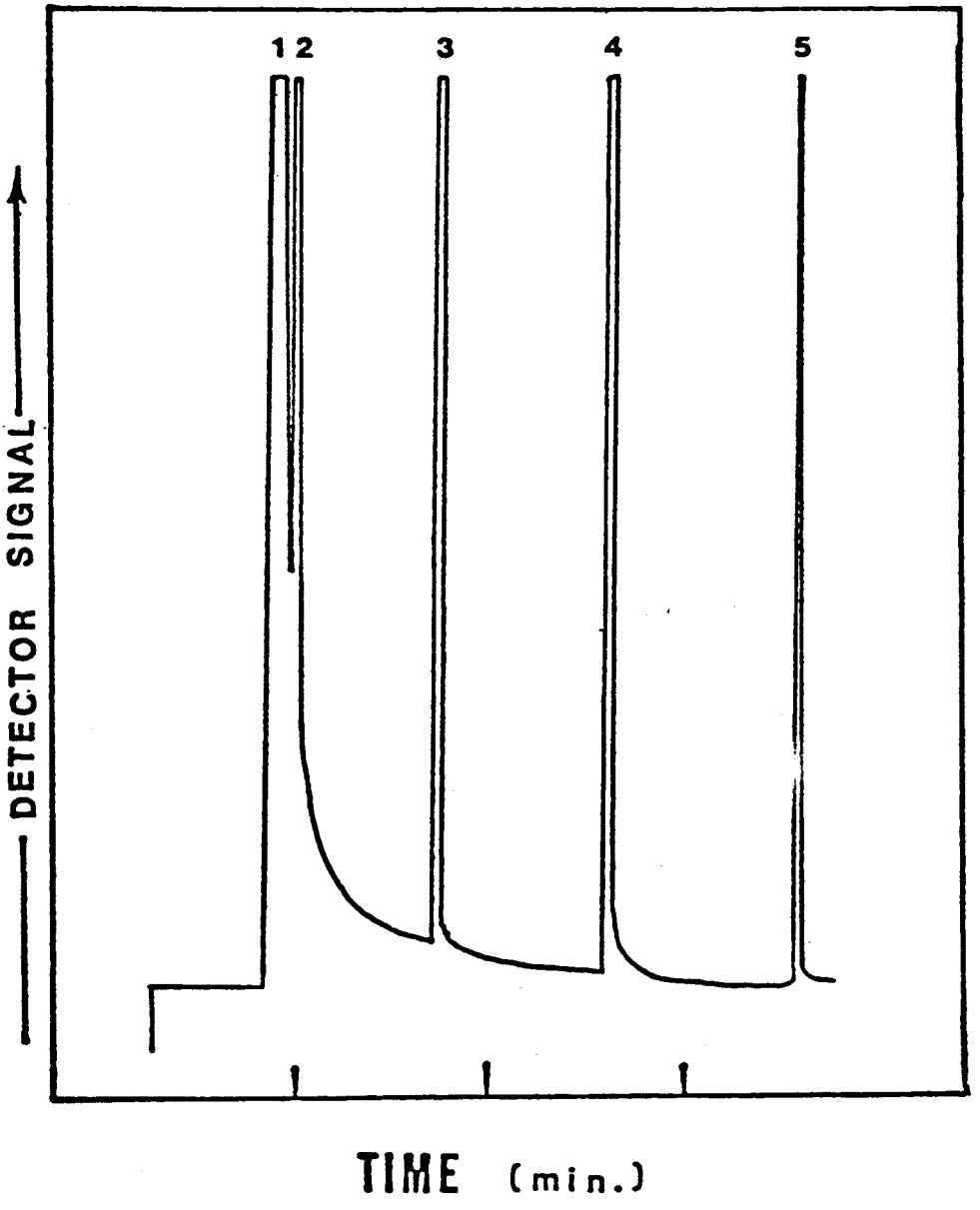

WIDE BORE BONDED METHYL SILICONE CAPILLARY COLUMN.

COMPONENT:

1. METHANOL
2. 2-PROPANOL
3. 3-METHYL-2-BUTANOL
4. 2-HEXANOL
5. METHYL CAPROATE

Figure X

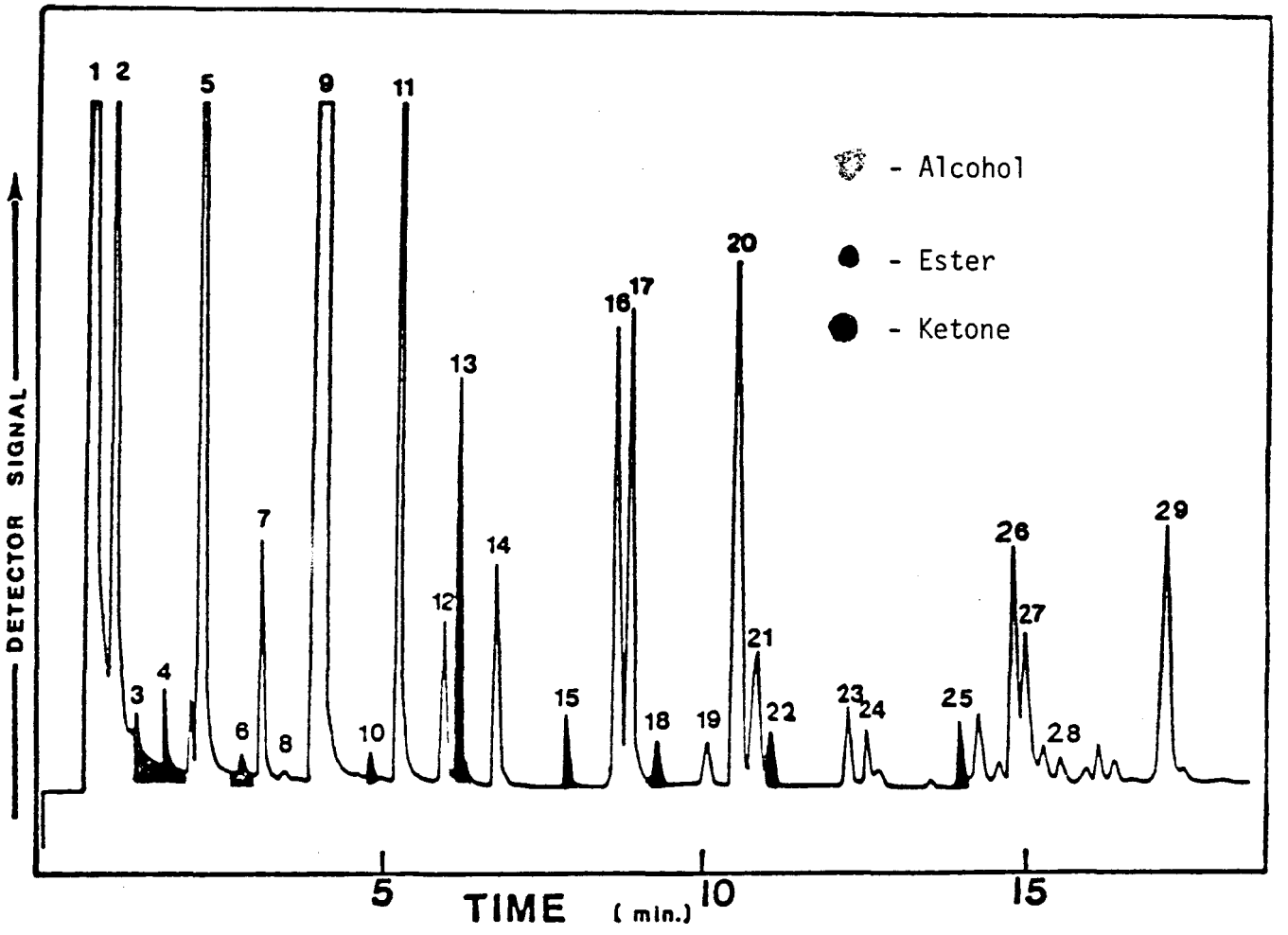

GAS CHROMATOGRAPH OF THE REACTOR PRODUCTS FOR HIGHER ALCOHOL SYNTHESIS FROM SYNTHESIS GAS (H_2/CO = 0.45) AT 8 l/hr, 290 °C, 75 ATM, AND PUMPING 2-METHYL-1-PROPANOL AT 5.0 μl/min. OVER THE CATALYST:

Cu/Zn/Cs THEORETICAL METAL MOLAR RATIO = 30/70/0.4
DOPED WITH CsOOCH AFTER CALCINATION.

COLUMN: BONDED METHYL SILICONE WIDE BORE CAPILLARY COLUMN.
TEMPERATURE PROGRAM: HOLD 25 SEC. AT 25 °C, THEN TO 100 °C AT 3.0 °C/min.

COMPONENTS:

1. METHANOL
2. ETHANOL
3. ETHYL FORMATE
4. METHYL ACETATE
5. PROPANOL
6. BUTYRALDEHYDE
7. 2-BUTANOL
8. ETHYL ACETATE
9. 2-METHYL-1-PROPANOL
10. 3-METHYL-2-BUTANONE
11. BUTANOL
12. 3-METHYL-2-BUTANOL
13. METHYL ISOBUTYRATE
14. 2-PENTANOL, 3-PENTANOL
15. METHYL BUTYRATE
16. 3-METHYL-1-BUTANOL
17. 2-METHYL-1-BUTANOL
18. 2-METHYL-3-PENTANONE
19. 4-METHYL-2-PENTANOL
20. PENTANOL
21. 2-METHYL-3-PENTANOL
22. 3-HEXANONE
23. 3-HEXANOL
24. 2-HEXANOL
25. METHYL PENTANOATE
26. 4-METHYL-1-PENTANOL
27. 2-ETHYL-1-BUTANOL
28. 3-METHYL-1-PENTANOL
29. HEXANOL

Figure XI

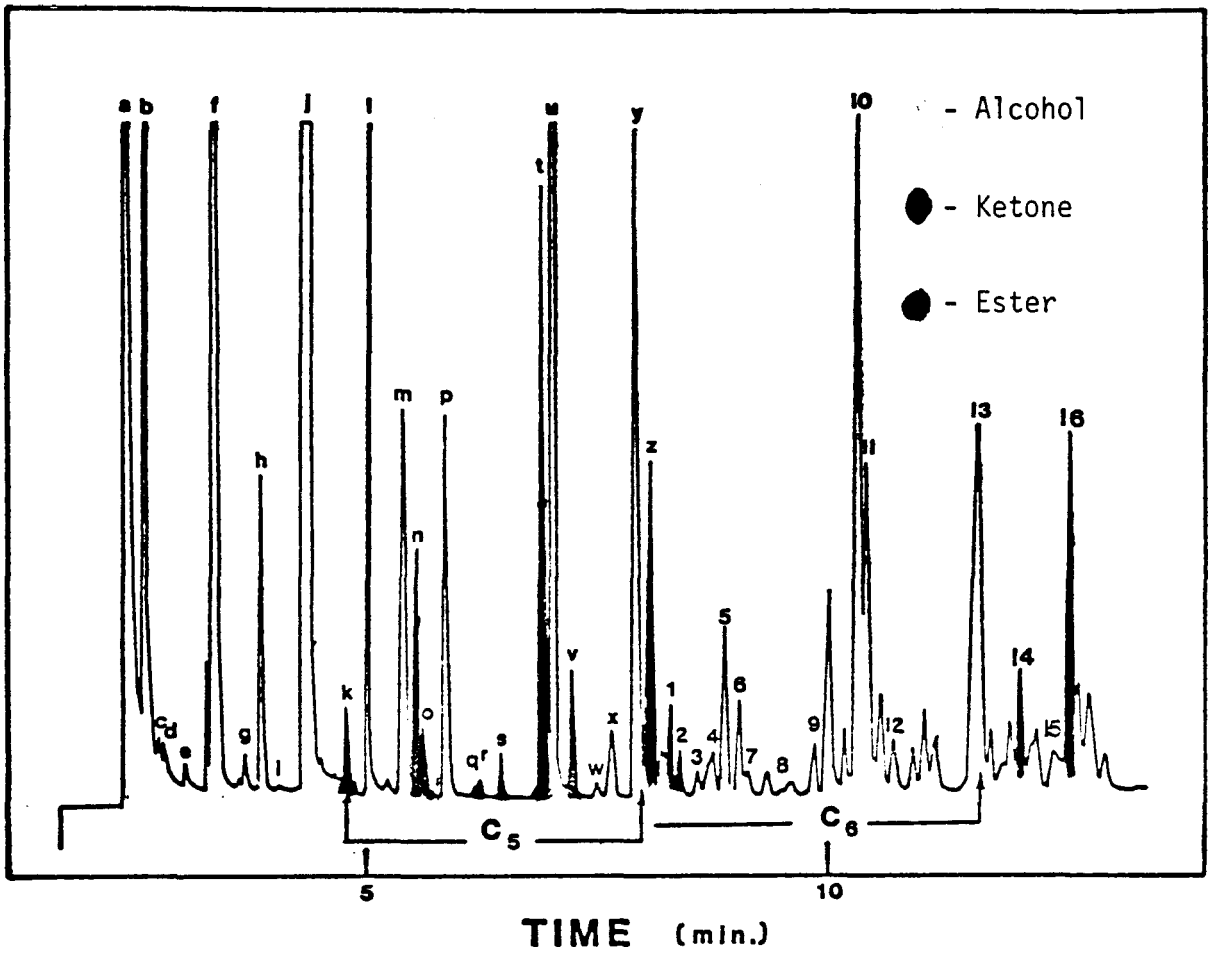

REACTOR PRODUCTS FOR HIGHER ALCOHOL SYNTHESIS FROM SYNTHESIS GAS (H_2/CO = 0.45) AT 309 °C, 75 ATM, AND PUMPING 2-METHYL-1-PROPANOL AT 5.0 µl/min. OVER Cu/Zn/Cs WITH A THEORETICAL MOLAR RATIO OF 30/70/0.4.
COLUMN: WIDE BORE BONDED METHYL SILICONE CAPILLARY COLUMN.

COMPONENTS:

A. METHANOL
B. ETHANOL
C. PROPIONALDEHYDE
D. ETHYL FORMATE
E. METHYL ACETATE
F. PROPANOL
G. BUTYRALDEHYDE
H. 2-BUTANOL
I. ETHYL ACETATE
J. 2-METHYL-1-PROPANOL
K. 3-METHYL-2-BUTANONE
L. BUTANOL
M. 3-METHYL-2-BUTANOL
N. METHYL ISOBUTYRATE
O. 3-PENTANONE
P. 2-PENTANOL, 3-PENTANOL
Q. ETHYL PROPIONATE
R. PROPYL ACETATE
S. METHYL BUTYRATE
T. 4-METHYL-2-PENTANONE
U. 3-METHYL-1-BUTANOL
2-METHYL-1-BUTANOL
V. 2-METHYL-3-PENTANONE
W. 2-METHYL VALERALDEHYDE
X. 4-METHYL-2-PENTANOL
Y. PENTANOL
Z. 2-METHYL-3-PENTANONE
1. 3-HEXANONE
2. 2-HEXANONE
3. 3-METHYL-2-PENTANOL
4. HEXANAL
5. 3-HEXANOL
6. 2-HEXANOL
7. ETHYL BUTANOATE
8. BUTYL ACETATE
9. METHYL PENTANOATE
10. 4-METHYL-1-PENTANOL
11. 2-ETHYL-1-BUTANOL
12. 3-METHYL-1-PENTANOL
13. HEXANOL
14. 2-HEPTANONE
15. 4-HEPTANOL
16. PROPYL BUTANOATE

that the wide bore bonded methyl silicone capillary column was able to separate higher alcohol products in the C_5 and C_6 region, making this a suitable column for total analysis of higher alcohol products.

Summary and Conclusion

The results presented here indicate that a wide bore capillary column with bonded methyl silicone as the stationary phase was able to separate and resolve the complex mistures of higher alcohol synthesis products formed over the Cs/Cu/ZnO catalysts. Optimum conditions were found for the column's performance, and these conditions can be used for quantitative analysis. Figures X and XI show that alcohols, esters, and ketones are major higher alcohol synthesis products. In order to complete this quantiative analysis method, samples will be spiked with known amounts of internal standards as references, and components will be compared to the references to account for the flame ionization detector's sensitivity to different components. The results will be compared with GC-mass spectroscopy and Fourier Transform infrared spectroscopy to eliminate any error in component identification.

APPENDIX

Method for Calculating Surface Concentrations of Dispersed Phases from XPS Intensities

Earlier we derived a method from Dreilings XPS intensity equations that is useful for comparing surface concentrations of alkali metals doped onto the surface of the Cu/ZnO catalyst (3). Inherent in the model was the assumption that the alkali was atomically dispersed. This allowed the approximation of the alkali XPS intensities to be independent of the escape depth, an advantage when comparing many different compounds for surface concentration. The model has been altered to allow the effects of alkali agglomeration, dispersion as a function of composition, and location of the alkali (over the Cu or ZnO phase) to be quantified.

The XPS intensity equations utilized to determine surface concentration and morphology are based on the relations by Dreiling (4). The system of interest consists of a bulk substrate, i, covered with an overlayer, j, of thickness z. The photoelectron intensities are given by equations A-1 and A-2,

$$\text{Substrate: } I_i = (k\sigma_i X_i^B g\lambda_i/E_i)(\exp -z/g\lambda_i) \qquad \text{(A-1)}$$

$$\text{Overlayer: } I_j = (k\sigma_j X_j^B g\lambda_j/E_j)(1-\exp -z/g\lambda_j) \qquad \text{(A-2)}$$

where k is an instrumental constant, σ is the photoionization cross section, g is the escape angular factor, X^B is the atomic volume concentration, and

λ is the escape depth of photoelectrons of kinetic energy E. The intensity equations contain the morphological information in the modifying exponential terms, where $\exp-(z/g\lambda_i)$ defines the attenuation of I_i by the overlayer and $(1-\exp-(z/g\lambda_j))$ the effect of overlayer thickness on I_j.

The bulk atomic densities are converted to surface densities by $X^S = X^B t^o$, where t^o is the monolayer thickness. The substrate intensity in equation A-1 accounts for attenuation from a continuous overlayer, while for partial coverages the effective overlayer thickness is defined by $t = zX_j^S/X_i^S$. Combining equations A-1 and A-2 with the above substitutions results in the relation,

$$\frac{I_j}{I_i} = \frac{X_j^S}{X_i^S}\left(\frac{\sigma_j\lambda_j E_i t_i^o}{\sigma_i\lambda_i E_j t_j^o}\right)\left(\frac{1-\exp-(z/g\lambda_j)}{\exp-(zX_j^S/X_i^S g\lambda_i)}\right) \qquad \text{(A-3)}$$

Equation A-3 gives the XPS intensity ratio of the overlayer to the substrate as a function of surface composition, particle dimension of the overlayer perpendicular to the substrate, and the degree of overlayer coverage (by the effective overlayer thickness). Applications, such as this, to determine particle sizes of dispersed phases have been successfully accomplished (5,6).

Application to Cs doped Cu/ZnO. The objective of the surface analysis in the Cs/Cu/ZnO system was to determine the dispersion of Cs as a function of the bulk Cs concentration, and to establish if the Cs was located over the Cu or ZnO phase. The approach was to compare the measured intensity ratio of Cs to Zn with values calculated for various surface morphologies.

In the case with Cs located over the ZnO phase, equation A-3 is used directly, where species j corresponds to Cs and i to Zn. Thus, X^S_{Cs} equals the number of surface Cs atoms, which is the total number of atoms for monolayer, half for a bilayer, etc., and X^S_{Zn} is the surface Zn atom density and is equal to $1.1744 \times 10^{19}\ S_{ZnO}$, with the quantity 1.1744×10^{19} Zn atoms/m^2 corresponding to the Zn surface density in the ZnO $(10\bar{1}0)$ crystal face, which is the predominant plane observed in these catalysts (7), and S_{ZnO} is the ZnO surface area. S_{ZnO} was determined from the total surface area, S_{Cat}, in conjunction with the Cu and ZnO particle sizes (d), in the following way. The surface area ratio of Cu to ZnO is proportional to the particle sizes by the relation, $S_{Cu}/S_{ZnO} = C(d_{ZnO}/d_{Cu})$, where C is a proportionality constant related to particle shape and the bulk concentration. From selective chemisorption studies of Parris et al. (8), $S_{Cu}/S_{ZnO} = (16\ m^2/g/(23\ m^2/g) = 0.6956$ for the Cu/ZnO = 30/70 mol% catalyst. Combining this result with the particle sizes of a freshly reduced catalyst, C is found to be 0.4657 and S_{ZnO} is then calculated by $S_{ZnO} = S_{Cat}/(1 + 0.4657\ d_{ZnO}/d_{Cu})$. The additional ancillary date necessary for equation A-3 can be found in Reference 3,

except for the escape depth of Cs. To be consistent with the earlier calculation of λ_{Zn}, the relationship given by Chang was again used (9), $\lambda = 0.2(E)^{1/2}t^{o}$, which for Cs equals 2.76 nm.

In the case with Cs located over the Cu phase, equation A-3 is used without the substrate attenuation term. To demonstrate the sensitivity of the XPS technique, examples of intensity changes resulting from different surface morphologies shall be given. The intensities are normalized to that calculated for a Cs monolayer over ZnO, see Figure A-1. The decrease in the intensity ratio for a Cs bilayer is 13%, which could be experimentally resolved. With larger particle sizes of the Cs phase, the intensity change would be easily distinguished. The decrease in the intensity ratio resulting from Cs over the Cu phase is a function of the bulk Cs concentration. For concentrations equal to or greater than 1 mol%, the effect is easily resolvable.

Figure A-1.

Theoretical plots of the Cs to Zn XPS intensity ratio for various Cs morphologies, normalized to the intensity ratio for a Cs monolayer coverage over ZnO.

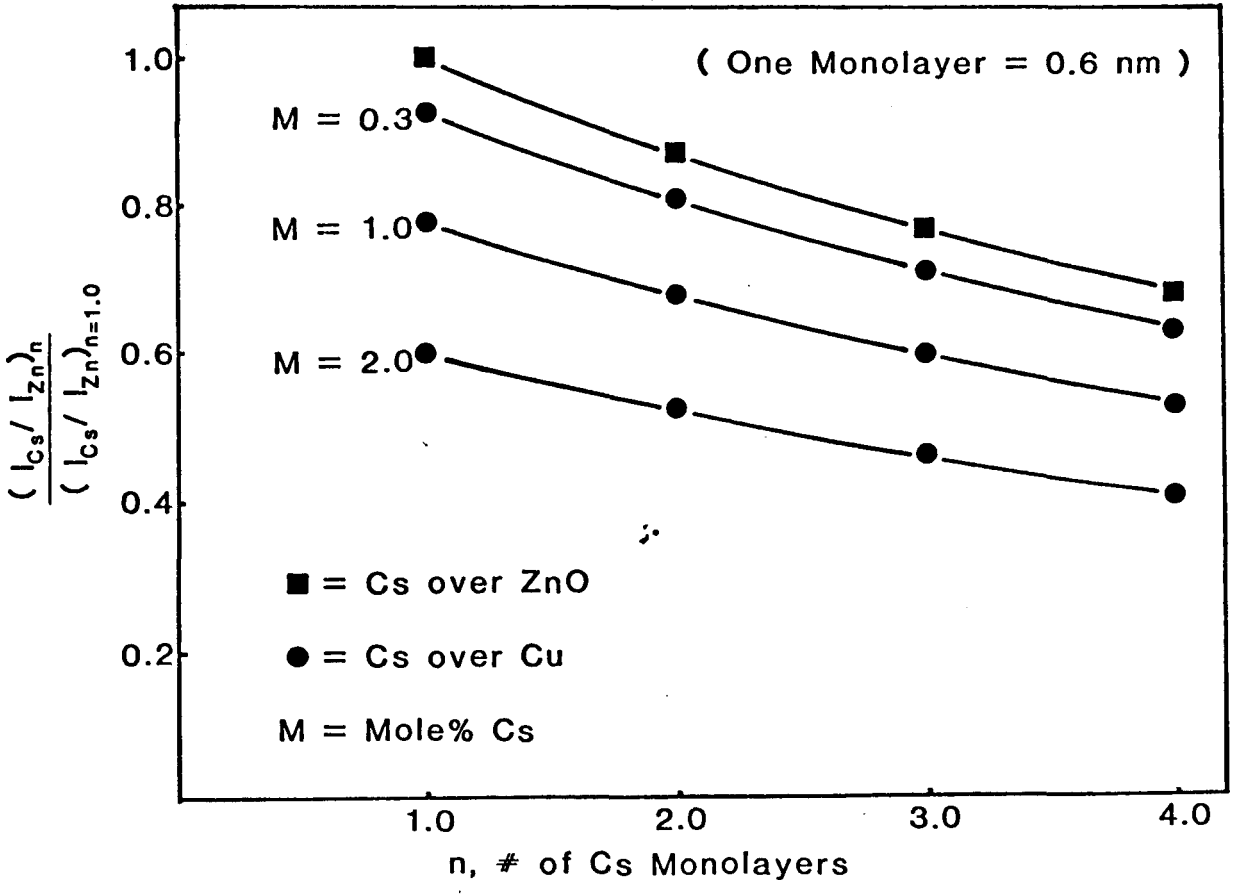

REFERENCES

1. Herman, R. G., Klier, K., Simmons, G. W., Finn, B. P., Bulko, J. B., and Kobylinski, T. P., J. Catal. 56, 407 (1979).

2. Anderson, J. R. "Structure of Metallic Catalysts", Academic Press, New York, N.Y., 365 (1975).

3. Vedage, G. A., Himelfarb, P. B., Simmons, G. W., and Klier, K., Preprint, Div. Pet. Chem., ACS, 28(5), 1261 (1983).

4. Dreiling, M. S., Surface Sci., 71, 231 (1978).

5. Kerkhof, F. P. J. M. and Moulijn, J. A., J. Phys. Chem., 83, 1612 (1979).

6. Fung, S. C., J. Catal., 58, 454 (1979).

7. Dominguez, J. M., Simmons, G. W., and Klier, K., J. Mol. Catal., 20, 369 (1983).

8. Parris, G. E. and Klier, K., Preprint, Div. Fuel Chem., ACS, 29(5), 226 (1984).

9. Chang, C. C., Surface Sci., 48, 9 (1975).

10. Trifiro, F., Vaccari, A., Busetto, C., Del Piero, G. and Manara, G., J. Catal., 85, 260 (1984).

11. Brocker, F. J., Marosi, L., Schroder, W., and Schwarzmann, M., German Patent 2,056,612 (May 31, 1972); assigned to BASF AG.

12. Courty, Ph. and Marcilly, Ch., in "Preparation of Catalysts III", (G. Poncelet, P. Grange and P. A. Jacobs, Eds.), p 485, Elsevier, Amsterdam, (1983).